Single Photon Emission Computed Tomography Tracer

7

Hans-Jürgen Pietzsch, Constantin Mamat, Cristina Müller, and Roger Schibli

Contents

H.-J. Pietzsch (✉) · C. Mamat
Helmholtz-Zentrum Dresden-Rossendorf (HZDR), Institute of Radiopharmaceutical Cancer Research, Dresden, Germany
e-mail: h.j.pietzsch@hzdr.de

C. Mamat
e-mail: c.mamat@hzdr.de

C. Müller · R. Schibli
Center for Radiopharmaceutical Sciences ETH-PSI-USZ, Paul Scherrer Institute, 5232, Villigen-PSI, Zürich, Switzerland
e-mail: cristina.mueller@psi.ch

R. Schibli
e-mail: roger.schibli@psi.ch

R. Schibli
Department of Chemistry and Applied Biosciences, ETH Zurich, 8093 Zurich, Switzerland

O. Schober et al. (eds.), *Molecular Imaging in Oncology*,
Recent Results in Cancer Research 216,
https://doi.org/10.1007/978-3-030-42618-7_7

7.1 Introduction

Single photon emission computed tomography (SPECT) and positron emission tomography (PET) are valuable molecular imaging modalities as both are capable of detecting minute amounts of radioactive tracer [232, 272]. Clinical PET is currently about 2–3 orders of magnitude more sensitive than SPECT, has a better spatial resolution, and offers superior quantification. Nowadays, many nuclear imaging centers possess PET or PET/CT scanners. However, the large infrastructure that is needed for the production of β^+-emitting radioisotopes (e.g., ^{18}F, ^{11}C, ^{64}Cu,^{68}Ga, ^{44}Sc) makes PET an expensive technology. At the moment, an approved clinical grade generator for PET radioisotopes is only available for ^{68}Ga. Hence, for routine application SPECT is still the state-of-the-art nuclear imaging modality because it is less expensive and can make use of a broader array of suitable and available radionuclides (Table 7.1). Importantly, SPECT imaging is a useful technology for monitoring targeted radionuclide therapy employing radioisotopes that emit—concomitantly with the therapeutic radiation—γ-rays of suitable energies for SPECT (e.g., ^{177}Lu, $^{188/186}$Re, ^{67}Cu, ^{131}I, ^{213}Bi) [10].

Generally, SPECT radiopharmaceuticals can be classified according to their biodistribution characteristics. There are those whose tissue distribution is determined exclusively by their chemical and physical properties and those whose distribution and accumulation are determined by their specific interaction with a biological target that is expressed at the site of interest (e.g., tumor-associated receptor) [24, 157]. Herein we focus on the development and (pre) clinical application of target-specific radiotracers. A target-specific SPECT radiopharmaceutical can be divided into two main parts: a targeting biomolecule and a γ-radiation-emitting radionuclide [157]. In the case of using radiometals as the radiation source, a bifunctional chelator is needed as an additional component of the radiopharmaceutical. Thus, a metallic radioisotope is coordinated by a suitable chelating agent that is conjugated to the targeting agent via a linker entity (Fig. 7.1). In a rational design of a SPECT tracer, the single components have to be critically

Table 7.1 Selection of radioisotopes for SPECT imaging (and therapy)

SPECT isotopes	Half-life	γ-Energy [keV]	
^{99m}Tc	6.02 h	141 (89%)	
^{111}In	2.80 d	171 (91%), 245 (94%)	
^{67}Ga	3.26 d	93 (39%), 185 (21%), 300 (17%), 394 (5%)	
^{123}I	13.22 h	159 (83%)	
^{125}I	59.41 d	35.5 (93%)	
^{155}Tb	5.32 d	87 (32%), 105 (25%)	
^{197m}Hg ^{197}Hg	23.8 h 64.1 h	134 (34%) 77 (19%), 279 (6%)	
Therapy/SPECT isotopes	Half-life	β^--Energy$_{average}$ [keV]	γ-Energy [keV]
^{177}Lu	6.65 d	134 (100%)	113 (10%), 208 (10%)
^{186}Re	3.72 d	347 (93%)	137 (9.5%)
^{188}Re	17.0 h	763 (100%)	155 (16%)
^{67}Cu	2.58 d	141 (100%)	185 (49%)
^{131}I	8.03 d	182 (100%)	365 (82%)

evaluated in order to achieve a balance among the demands of an adequate target binding and a rapid excretion.

The majority of diagnostic radiopharmaceuticals currently available in nuclear medicine make use of metallic radioisotopes. For SPECT imaging, technetium-99m is the most widely applied radioisotope because of its ideal physical decay properties and easy availability by a generator system (Table 7.1). Indium-111 is another SPECT radioisotope frequently used in the clinics where it is often employed as a surrogate for yttrium-90 analogs since ^{90}Y that is used for therapeutic purposes is a pure β^--emitter. In contrast, clinical application of gallium-67 is relatively rare. Non-metallic radionuclides used for SPECT are basically the isotopes of iodine. Iodine-123 is the preferred isotope for imaging purposes (Table 7.1) due to its dosimetry and imaging characteristics that are superior to iodine-131 and iodine-125.

A targeting biomolecule serves as a "carrier" for specific delivery of the radionuclide to the target-expressing cells of interest. Such biomolecules could be biomacromolecules like specific antibodies (or antibody fragments) or small-molecular-weight molecules (e.g., peptides, vitamins, nucleosides). Each class of targeting agents has its pros and cons for its use in diagnostic nuclear medicine and for a potential translation to therapeutic applications. Peptide-based radiopharmaceuticals represent by far the largest group of tumor-targeted nuclear imaging agents currently in use.

During tracer development, the first steps are based on chemistry and molecular biology methods such as peptide syntheses, conventional or combinatorial chemistry, and phage display techniques for preparation, identification, and isolation of high-affinity binders to a particular receptor. Determination of the tumor-targeted radiotracer's stability in vitro and its ability to bind with high affinity to the target

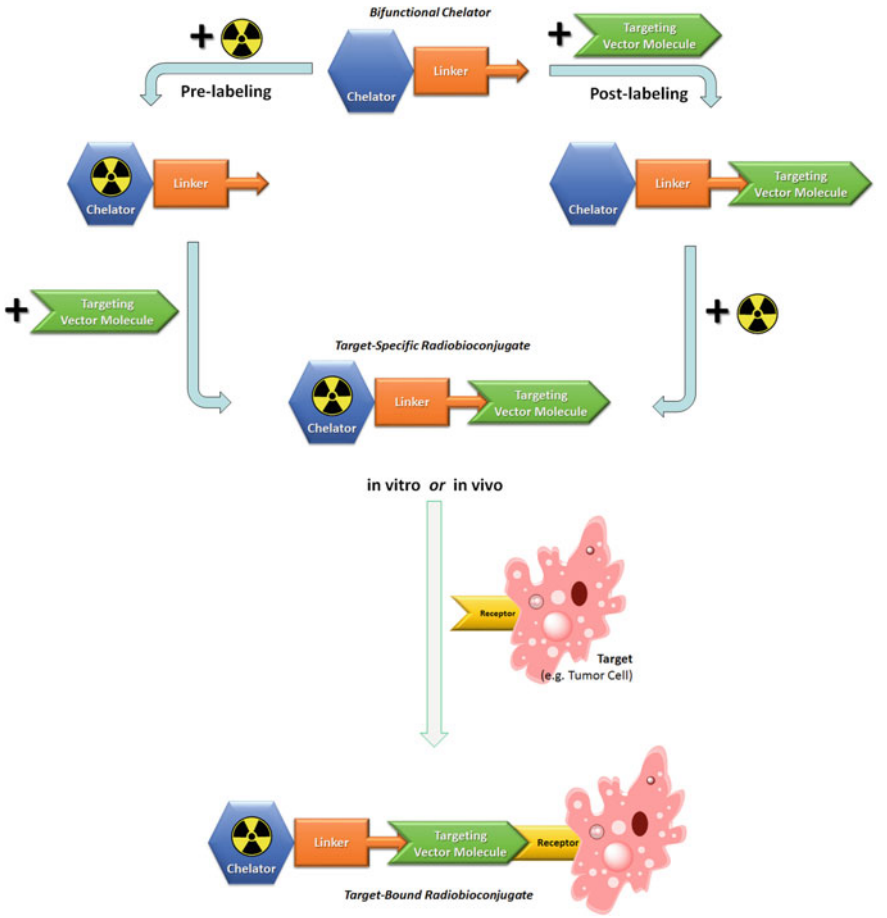

Fig. 7.1 Schematic representation of a biomolecule (targeting vector molecule) that is conjugated to a radiometal. The bifunctional chelator that is conjugated to the target-specific biomolecule is necessary for coordination of the radiometal. Two strategies are possible to conjugate the biomolecules to the chelator and the radionuclide: pre-labeling and post-labeling. After radiolabeling, the target-specific radiobioconjugate was intraveniously administered, binds to the tumor cell surface-associated target (e.g., receptor) and allows visualization of target-expressing malignant lesions via SPECT

structure on cultured cancer cells are the first requirements in this early development stage. The in vitro evaluation is followed by investigations in vivo using an adequate animal model, typically tumor-bearing small rodents. It is important to recognize that radiolabeled tumor imaging agents display different biodistributions and pharmacokinetics in animal models compared to humans due to a different metabolism, differences in the volume of distribution, and potential cross-reactivity of the targeting entity with normal tissues expressing the target receptor or antigen

in humans [42]. Significant variability in the tissue distribution of radiotracers might occur among different animal models (e.g., mice vs. rats) or different animal strains (e.g., nude mice vs. normal mice). However, small rodents have emerged as generally the most useful and cost-effective animal models for developing and evaluating radiotracers and to test new experimental approaches to increase their localization in tumors. Postmortem biodistribution studies allow the detection and quantification of a cumulated activity portion in targeted and non-targeted tissues, and thus the determination of the radiotracer's pharmacokinetic profile. Collection of blood and tissue samples for identification of metabolites at different time points after radiotracer application provides information about the radiotracer's circulation time and it is in vivo stability. By increasing the availability of small-animal SPECT and SPECT/CT scanners in recent years, the process of radiotracer development has been significantly improved and accelerated while the number of test animals required has been reduced. Thus, a wide variety of targeted SPECT radiotracers are currently being developed and preclinically tested for imaging of various tumor types expressing one or more of the most relevant receptor types [247].

The focus of this chapter is to present general aspects for the design of SPECT tracers followed by specific examples of recent SPECT imaging agents based on biomacromolecules like antibodies, antibody fragments, proteins as well as other small-molecular-weight biomolecules such as peptides, vitamins, or nucleosides referred to as vector molecules. The examples demonstrate possibilities for optimization of the tracer design by tuning single components of these imaging agents. Finally, potential causes for failures in SPECT tracer design are discussed.

7.2 General Aspects for the Design of SPECT Tracers

The ideal SPECT tracer exhibits excellent tissue penetration, high affinity to the target structure, specific uptake and retention in the target cells, and rapid clearance from non-targeted tissues and organs. In addition, it is highly stable in vivo, easy to prepare, and safe for human application. These aspects are crucial because injected radiotracers that are not stable, not bound to the target, or not rapidly excreted create high background signals resulting in low tumor-to-background contrast, false positive results, and unnecessary radiation dose burden to the patient [10].

In the case of metallic radioisotopes, a bifunctional chelator is needed that is covalently linked to a biomolecule [157]. Since the stability of the radiometal complex is a critical aspect for the success of a radiopharmaceutical, it is important to choose an ideal chelating system that allows the formation of radiometal complexes of high thermodynamic stability and kinetic inertness [24]. Among the SPECT isotopes currently in use, technetium-99m is still the workhorse of diagnostic nuclear medicine. It is used in the majority of diagnostic scans conducted each year in hospitals worldwide. The preferred use of ^{99m}Tc-radiopharmaceuticals reflects the ideal nuclear properties of the isotope and, until recently, the convenient availability from commercial ^{99}Mo/^{99m}Tc-generators.

Technetium is a transition metal that presents a major challenge with respect to designing radiopharmaceuticals with favorable in vivo properties. In order to link the radionuclide to a targeting molecule, [^{99m}Tc]pertechnetate with Tc in the oxidation state +VII that is eluted from the ^{99}Mo/^{99m}Tc-generator must be reduced to build a complex with an appropriate bifunctional chelating system, most commonly in the oxidation state +I, +III or +V. The ^{99m}Tc(V)-oxo and ^{99m}Tc(V)-organohydrazino cores are most extensively studied (Fig. 7.2). The ^{99m}Tc(V)-oxo-core generally adopts a square-pyrimidal geometry with the π-bonding oxo-group in the apical position. The core is stabilized by σ- and π-donating groups where amino, amido, and thiolate ligands as well as tetradentate ligands of the N_xS_{4-x}-class have been investigated [24, 157, 211]. A prominent example of a tetradentate chelator is the peptide-based chelator mercapto-acetylglycylglyclgylcine (H_5MAG_3) [150].

An alternative approach is the use of the ^{99m}Tc(V)-organohydrazino nicotinamide (HYNIC) core that was first introduced by Abrams et al. 20 years ago [1, 250]. The advantages of this system are the facile functionalization of targeting entities via amide linkage. It has therefore been used for ^{99m}Tc-labeling of a variety of high, medium, and small-molecular weight biomolecules [65, 66, 83, 107, 161, 235, 274, 279, 296]. Since the HYNIC chelator can only occupy one or two coordination sites on the metal center, co-ligands such as tricine are needed to complete the coordination sphere of ^{99m}Tc [74, 160, 219]. The possibility for selection of appropriate co-ligands is advantageous for an easy modulation of the hydrophilicity and pharmacokinetics of the ^{99m}Tc-HYNIC-derivatized biomolecules. However, the presence of multiple species in solution due to different bonding modalities of the HYNIC moiety and co-ligands might be problematic for a commercial development, because of the increasing regulatory hurdles and the requirements of fully characterized products.

Another, less frequently employed approach is the use of a ^{99m}Tc(V)-dioxo-core coordinated by nitrogen ligands that form octahedral complexes with the oxygens *trans* to each other [129]. The group of Nock and Maina made successful use of a tetraamine chelator for ^{99m}Tc-radiolabeling of several peptide-based biomolecules forming monocationic polar complexes with the ^{99m}Tc(V)-dioxo core [171, 205, 207]. The advantages of this radiolabeling strategy include its easy formation at

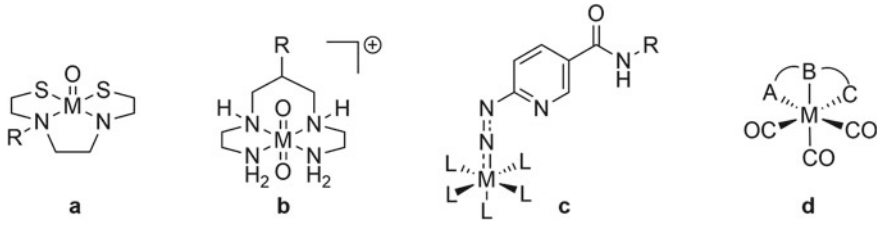

Fig. 7.2 The most frequently used ^{99m}Tc-complexes for radiobioconjugates. **a** ^{99m}Tc(V)oxo core, **b** ^{99m}Tc(V)dioxo core, **c** ^{99m}Tc(V)organohydrazino nicotinamide (HYNIC) core, and **d** ^{99m}Tc(I)-tricarbonyl core. M = ^{99m}Tc, L = co-ligands

ambient temperature, its high stability in the biological milieu, and considerable hydrophilicity.

A completely different ^{99m}Tc-radiolabeling strategy has been introduced by the development of the tricarbonyl technique which offered new opportunities for the design of ^{99m}Tc(I)-radiotracers [6–9, 75, 76, 240, 241]. The water-soluble ^{99m}Tc(I)-tricarbonyl precursor's aqua ligands are readily exchanged allowing the coordination of preferentially tridentate chelators that can be modified to provide complexes with cationic, neutral, or anionic overall charge [92, 174, 194, 216, 240, 251]. In addition, the tricarbonyl radiolabeling strategy is also accessible for the preparation of stable radiometal complexes using β-particle-emitting rhenium isotopes ($^{186/188}$Re, Table 7.1). Hence, the production of isostructural compounds with the "matched pair" ^{99m}Tc/$^{188/186}$Re for diagnostic and therapeutic purposes has become feasible thanks to the tricarbonyl strategy, a feature which is often not fulfilled with Re(V) complexes [195].

Radiolanthanides (e.g., ^{177}Lu) and lanthanide-like isotopes as well as indium and gallium are used in the oxidation state +III. They can generally be coordinated by polyaminopolycarboxy chelating systems. Coordination numbers of lanthanides are typically between seven and ten whereas coordination numbers of eight or nine are most common in Ln(III) complexes with polydentate chelators. The 1,4,7,10-tetraazacyclododecane-1,4,7,10-tetraacetic acid (DOTA) chelator emerged as particularly useful for lanthanide coordination of therapeutic radiopharmaceuticals because of the formation of metal complexes of extremely high thermodynamic stability and kinetic inertness (Fig. 7.3). In addition, the hydrophilic acetate chelating arms of DOTA favor a fast clearance of radiotracers from the blood and non-targeted organs and tissues. Despite the similarities of the SPECT radioisotopes gallium-67 and indium-111 they are different in size, coordination number, and charge density. Ga^{3+} has a small ionic radius (0.65 Å) and the coordination number is six whereas the ionic radius of In^{3+} is larger (0.92 Å) and it is seven- or eight-coordinated in its complexes. The structural differences among Ga and In complexes might have an influence on the overall tissue distribution of one and the same bioconjugate as recently exemplified with a somatostatin analog [114]. A higher tumor uptake and a lower kidney retention have been reported for ^{67}Ga-DOTATOC compared to that of ^{111}In-DOTATOC. Whereas DOTA appears to be an ideal chelator for coordination of lanthanide (radio)isotopes like Lu^{3+} or In^{3+}, its coordination cavity is not ideal for Ga^{3+} as it is too large. On the other hand, there is a perfect fit between the size of Ga^{3+} and the coordination cavity formed by the N_3O_3 donor atoms of the macrocyclic 1,4,7-triazacyclononane-1,4,7-triacetic acid (NOTA) chelator [157]. Consequently, a higher thermodynamic stability constant has been found for Ga-NOTA complexes compared to those of Ga-DOTA-complexes [67]. In some cases, open chelating systems are more favorable than macrocycles because they are capable to form radiometal complexes at ambient temperature which is particularly important for temperature-sensitive targeting agents. Examples are variable versions of diethylenetriamine pentaacetic acid (DTPA, CHX-A″-DTPA, etc., Fig. 7.3). DTPA is one of the most commonly employed acyclic ligands in radiochemistry useful for coordination of ^{111}In, ^{67}Ga,

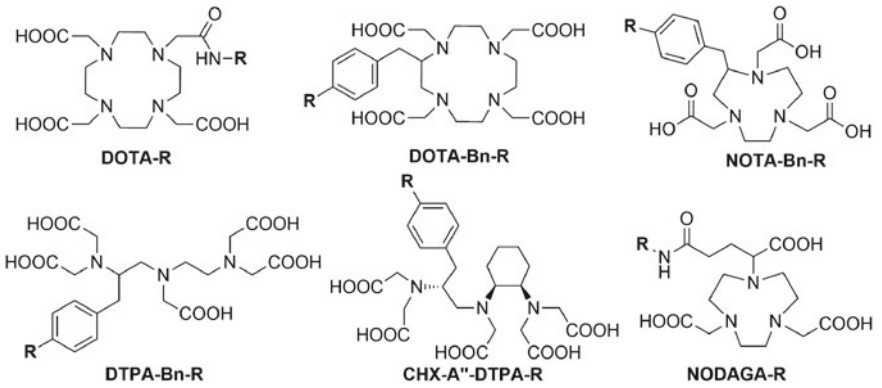

Fig. 7.3 The most frequently used macrocyclic (DOTA, NOTA) and acyclic (DTPA) chelators for complexation of radioisotopes for SPECT imaging (e.g., ^{111}In, ^{67}Ga) and combined therapy/SPECT imaging (e.g., ^{177}Lu)

and radiolanthanides. For ^{111}In-complexation DTPA emerged as the ideal chelating agent [173].

In addition to the bifunctional chelator's function for stable coordination of the radiometal, the linker entity is important for conjugation with the biomolecule and might influence the overall pharmacokinetics of the radiopharmaceutical. By affecting the biomolecule's lipophilic or hydrophilic characteristics the linker system can serve for controlling its in vivo behavior. Thus, the nature of a bifunctional chelator in terms of geometry, lipophilicity, and overall charge plays a crucial role in determining the biodistribution of (tumor-) targeted radiopharmaceuticals [24].

Functionalization of amino acid side chains (e.g., lysine, cysteine) with chemically reactive probes of bifunctional chelators is a largely uncontrolled random process that results in a heterogeneous mixture of conjugates modified at variable sites. A considerable advantage of small-molecular weight biomolecules (e.g., peptides and vitamins) is the fact that derivatization with a bifunctional chelating agent can be governed by specific chemical reactions that yield a single, clearly defined species. In contrast, loss of binding affinity is of concern during the process of antibody derivatization because modification of the Fab region (antigen-binding site) can possibly have deleterious effects on the target binding of the protein. Both loss of binding activity to the target and overlabeling effects are highly undesired processes because they result in unwanted background radiation and unspecific accumulation of the antibody radioconjugates in the liver. For this reason, recent endeavors were undertaken for the development of site-specific derivatization via enzymatic reactions that are selective for a particular amino acid [128, 185] or sugar residue [34] at a specified site of the antibody.

Since small-molecular-weight molecules are usually stable at a broad range of temperatures and pH values, the radiolabeling procedure is mostly smooth and quantitative. In contrast, proteins are generally sensitive to elevated temperatures.

Thus, commonly applied methods for radiometal-labeling of proteins are time-consuming due to the low reaction temperature applicable. To overcome this drawback, pre-labeling strategies have been proposed allowing the preparation of radioimmunoconjugates within a shorter period of time while preventing the risk of affecting the antibody's scaffold under possibly harsh conditions needed for direct radiolabeling strategies [153, 302].

7.3 Peptide-Receptor Radionuclide Imaging

Since receptors for regulatory peptides are overexpressed in a variety of human cancers, it is a prominent strategy to use radiolabeled analogs of these physiologically occurring peptides for tumor-targeted nuclear imaging. Advantages of using peptides are their good tissue penetration, a fast clearance, and minimal immunogenicity [247]. Small peptides of usually less than 40 amino acid residues are easily accessible through solid-phase peptide synthesis. Their tolerance toward bulky modification and resistance toward harsh chemical conditions that are sometimes inevitable during radiolabeling procedures are further advantages. Importantly, a formulation of a radiolabeled peptide consists of identical molecules with a well-defined structure. Clearly, the most outstanding example of success in the field of peptide-based diagnostic and therapeutic nuclear medicine has been the use of somatostatin analogs for targeting the somatostatin receptor [144]. Somatostatin-derived tracers designed to image somatostatin receptor subtype 2 (sst2)-expressing tumors have enjoyed almost two decades of successful preclinical development and extensive clinical application. This example has paved the path for further exploration of radiolabeled peptides targeting other tumor-associated receptors such as gastrin-releasing peptide receptors, neurotensin receptors, or cholecystokinin receptors [29, 225].

7.3.1 Somatostatin Analogs

The prototypes of radiolabeled peptides for SPECT imaging are the somatostatin analogs commonly labeled with ^{111}In or ^{99m}Tc. Somatostatin receptors are overexpressed on neuroendocrine tumors including pituitary adenomas, pheochromocytomas, paragangliomas, neuroblastomas, and medullary thyroid cancers. From the five subtypes of somatostatin receptors belonging to the G-protein coupled receptors, subtype 2 is the most widely overexpressed form in neuroendocrine tumors. In the beginning of their development, somatostatin analogs suffered from rapid degradation in vivo. Such limitations have been overcome by stabilization strategies through the development of synthetic peptides. Peptides of high chemical stability became accessible by introduction of D-amino acids or other unnatural amino acids at known cleavage sites, cyclization, or modification of C- and N-termini via amidation, reduction, alkylation, or acylation [247]. The clinically

approved ^{111}In-labeled DTPA^{0}-octreotide (OctreoScan) has proven to be a successful and versatile molecular imaging agent (Figs. 7.4 and 7.5). The most frequently used DOTA-coupled, somatostatin-based peptides are [DOTA^{0}, Tyr^{3}]-octreotide and [DOTA^{0}, Tyr^{3}, Thr^{8}]-octreotate usually referred as DOTATOC and DOTATATE (Fig. 7.4). These analogs have also been successfully employed for therapeutic purposes when radiolabeled with particle-emitting radioiosopes (e.g., ^{177}Lu, ^{90}Y). Several sst2-binding somatostatin analogs are currently used in the clinic. Further research projects are focusing on the development of new and improved somatostatin analogs with a broader receptor subtype affinity profile. Such compounds would extend the range of targeted cancer candidates and increase the net tumor uptake when several receptor subtypes are expressed on the same tumor cell [112, 184].

Although [^{111}In]In-DTPA-(D-Phe^{1})-octreotide proved to be reliable for the detection of neuroendocrine tumors (NET), the potential clinical advantage of ^{99m}Tc-labeling in comparison to radiolabeling with ^{111}In led to the development of ^{99m}Tc-labeled somatostatin analogs. [^{99m}Tc]Tc-EDDA-HYNIC-TOC (^{99m}Tc-Tektrotyd) is a radiopharmaceutical indicated for diagnosis of tumors with overexpression of SSTR, especially subtype 2 (SSTR2) [15, 90, 143, 285].

The complex formation requires the use of a coligand such as tricine or ethylenediamine diacetic acid (EDDA). The coordination mode of HYNIC with ^{99m}Tc is not known exactly. Usually, a monodentate “end-on”-N=N- coordination is proposed (Fig. 7.4).

The generally high kidney uptake of radiometallated peptides due to their reabsorption in the renal proximal tubules is a drawback for peptide-based tumor targeting as it may lead to reduced contrast and quality of diagnostic imaging and damage radiosensitive kidneys if applied for therapeutic purposes [104]. Thus, several strategies to reduce tubular reabsorption of peptidic radiotracers have been investigated. One strategy relies on the chemical modification of the peptide with entities or overall charges that would potentially reduce renal uptake. A successful example of such modification is given by the work of Schwaiger and co-workers who developed ^{125}I-somatostatin analogs modified with carbohydrate entities [248, 305]. Glycation modified the physicochemical behavior of the radiotracers in that pharmacokinetics were significantly improved as shown by reduced hepatic uptake and biliary excretion and a rapid clearance from the circulation via the kidneys without increasing renal accumulation of radioactivity. Another approach is based on the administration of additional substances for potential inhibition of peptide reabsorption. In this respect the co-infusion of the cationic amino acids lysine and arginine is the most prominent example since this combination successfully reduced renal accumulation of radiolabeled somatostatin analogs in preclinical studies [31, 61, 294] and in patients [111, 229].

Originally, it was proposed that peptide agonists that are efficiently internalized into receptor-expressing cancer cells would be the best candidates for tumor imaging [48]. However, the two somatostatin analogs ^{111}In-DOTA-sst2-ANT and ^{111}In-DOTA-sst3-ODN-8 showed extremely high tumor accumulation despite being receptor antagonists [100]. It could be shown in vitro that a more than 15-fold

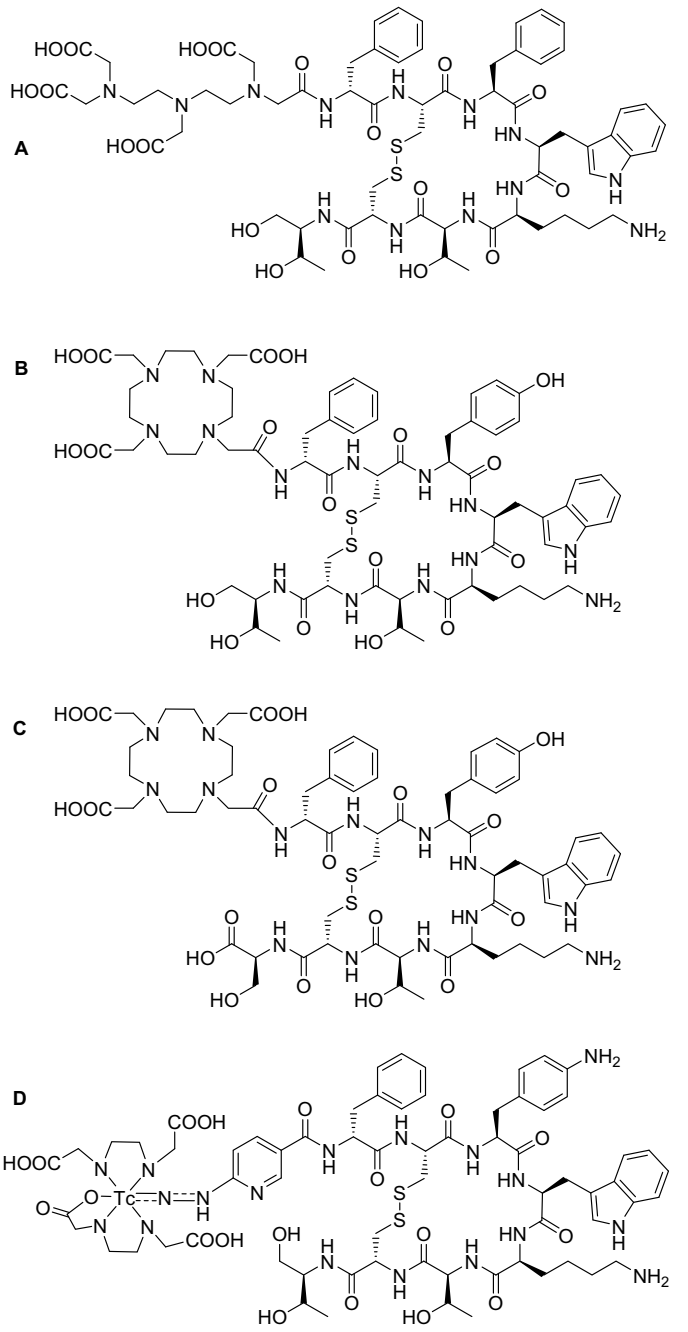

Fig. 7.4 Chemical structures of DTPA- and DOTA-modified somatostatin analogs for targeted diagnosis and therapy of somatostatin receptor-positive cancer diseases. **a** $DTPA^0$-octreotide, **b** $DOTA^0$-Tyr^3-octreotide (DOTATOC), **c** $DOTA^0$-Tyr^3-Thr^8-octreotate (DOTATATE), **d** [^{99m}Tc] Tc-EDDA-HYNIC-TOC (^{99m}Tc-Tektrotyd)

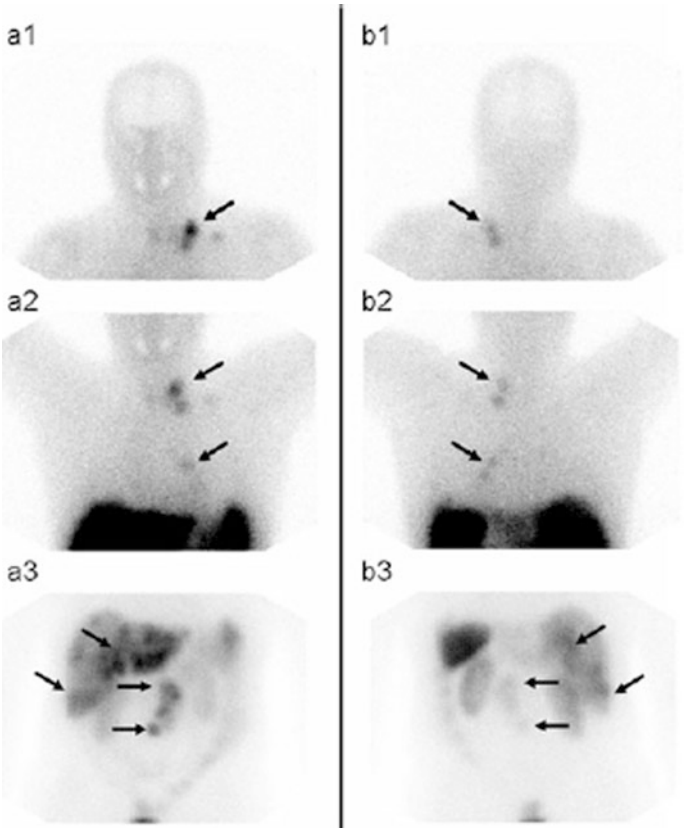

Fig. 7.5 Scintigraphy [multiple planar spot views, anterior **a** and posterior **b** of the head/neck (1), thorax (2), and abdomen (3)] performed 24 h after injection of ^{111}In-octreotide (OctreoScan; Covidien, Petten, the Netherlands) in a patient diagnosed with a well-differentiated endocrine carcinoma (carcinoid) with lymphogenic spread in the abdomen and supraclavicular and multiple metastatic lesions in the liver and lungs. The images have been kindly provided by J.J.M. Teunissen (MD, Ph.D.), Erasmus Medical Center, Rotterdam, The Netherlands

increased number of binding sites per cell were accessible for antagonists compared to their agonist analogs and in addition slow ligand dissociation from the receptor was determined. These findings attracted the attention of many research groups and led to the development of further sst2-binding somatostatin-based antagonists. The studies confirmed that high-affinity somatostatin receptor antagonists that poorly internalize in tumor cells exhibit improved tumor-targeting characteristics than corresponding agonists. The fact that this phenomenon was found not only for sst2-selective compounds but also for sst3-selective compounds suggests that this phenomenon is valid for more than just one particular receptor [47].

7.3.2 Bombesin Analogs

The bombesin receptor family comprises four receptor subtypes whereof the gastrin-releasing peptide (GRP) receptor or bombesin receptor subtype 2 (BB2) has been studied most thoroughly [268, 269]. The impetus for targeting the GRP receptor is based on the fact that a variety of human tumors overexpress GRP receptors including prostate, breast, and small cell lung cancers [106, 177, 187, 256]. The development of ^{99m}Tc- and ^{111}In-bombesin analogs has been the focus in recent years in many research laboratories (Table 7.2) [20, 206, 288]. De Barros and colleagues presented a BBN-kit using HYNIC and EDDA as chelating source for ^{99m}Tc [59]. A detailed summary was published by Moreno et al. in 2016 [188]. The tricarbonyl technique, which was developed in view of the opportunity to use ^{99m}Tc and ^{188}Re as matched pair for diagnosis and therapy [6, 242], has been employed most extensively for radiolabeling of bombesin analogs [85, 86, 91–93, 145, 226, 230, 251, 266, 267, 317]. A drawback of this strategy is, however, the fact that the most ^{99m}Tc/^{188}Re-tricarbonyl-based bombesin derivatives are predominantly cleared via the hepatobiliary excretion pathway because of the tricarbonyl's inherent lipophilicity [64]. Increasing the hydrophilicity of radiolabeled GRP-targeting peptide conjugates is necessary because accumulation of radioactivity in the liver and intestinal tract would compromise their capacity to effectively image solid tumors and metastatic lesions in the abdomen. This has been accomplished, for example, by introduction of "innocent" peptide sequences such as polylysine, polyglycine, or polyaspartic acid residues [159]. Additionally, it was shown that the introduction of a polar serylserylserine spacer into ^{99m}Tc-tricarbonyl pyrazolyl bombesin analogs resulted in a longer retention time of the radiotracer in the tumor tissue compared to analogs with more lipophilic linker entities consisting of β-alanine or triglycine [12]. Based on the promising results experienced with somatostatin analogs conjugated to carbohydrates [230, 248, 305], glycation of bombesin tracers was approached with the aim to increase their overall hydrophilicity [251]. In this respect Garcia et al. tested three different bombesin analogs in vitro and in vivo. One of the derivatives was modified with a linker bearing a lysine that was coupled to the glycomimetic shikimic acid at the ε-amino group. Another bombesin derivative was glycated via an Amadori rearrangement and the third compound was a bombesin analog derivatized with an azido-glucose that was connected to an alkyne-functionalized linker entity via the Cu-catalyzed click reaction (Table 7.2). The introduction of polar carbohydrates had no negative effects on the in vitro stability and the internalization or efflux profile of the radiotracers in cultured tumor cells. In contrast, these modifications led to a significant reduction in abdominal radiotracer accumulation, a clearly higher tumor uptake, and thus improved tumor-to-background ratios in vivo. The best results were obtained with the bombesin analog modified via a "click" reaction that contained a triazole-coupled glucose entity. The tissue distribution could be clearly ameliorated as demonstrated via SPECT/CT imaging studies where the tumor uptake was shown to be increased (Fig. 7.6).

Table 7.2 Sequence of various bombesin analogs

Analog	Chelator	Linker			
			1–6	7–13	14
Bombesin			pGlu-Gln-Arg-Leu-Gly-Asn-	-Gln-Trp-Ala-Val-Gly-His-Leu-	-Met-NH_2
Demobesin-1	N4	-BzDig-	-**DPhe**-	-Gln-Trp-Ala-Val-Gly-His-Leu-**NHEt**	
$KBBN_{50}$	HYNIC	-βAla-		-Gln-Trp-Ala-Val-Gly-His-Leu-	-Met-NH_2
BBS-1	(N^{α}His)Ac-	-βAla-βAla-		-Gln-Trp-Ala-Val-Gly-His-**Nle**-	
BBS-2	(N^{α}His)Ac-	**Lys**(**sha**)-βAla-βAla-		-Gln-Trp-Ala-Val-Gly-His-**Nle**-	
BBS-3	(N^{α}His)Ac-	-**Lys**(**Amd**)-βAla-βAla-		-Gln-Trp-Ala-Val-Gly-His-**Nle**-	
BBS-4	(N^{α}His)Ac-	-Ala(^{N}**TG**)-βAla-βAla-		-Gln-Trp-Ala-Val-Gly-His-**Nle**-	
MP2653	DTPA		-**aCMpip**-**Tha**-	-Gln-Trp-Ala-Val-**βAla**-His-**Tha**-	-**Nle**-**NH_2**
MP2346	DOTA		-**Pro**-Gln-Arg-**Tyr**-Gly-Asn-	-Gln-Trp-Ala-Val-Gly-His-Leu-	-Met-NH_2
Pesin	DOTA	-$dPEG_4$-		-Gln-Trp-Ala-Val-Gly-His-Leu-	-Met-NH_2
AMBA	DOTA	-CH_2CO-Gly-(4-aminobenzoyl)-		-Gln-Trp-Ala-Val-Gly-His-Leu-	-Met-NH_2
RM 1	DOTA	-CH_2CO-Gly-(4-aminobenzoyl)-	-**Phe**-	-Gln-Trp-Ala-Val-Gly-His-**Sta**-	-**Leu**-NH_2

Lys(sha) = lysine-coupled shikimic acid, Lys(Amd) = Amadori Product; Ala(^{N}TG) = triazole-coupled glucose, Sta = statyl (*3S,4S*-4-amino-3-hydroxy-6-methylheptanoyl)

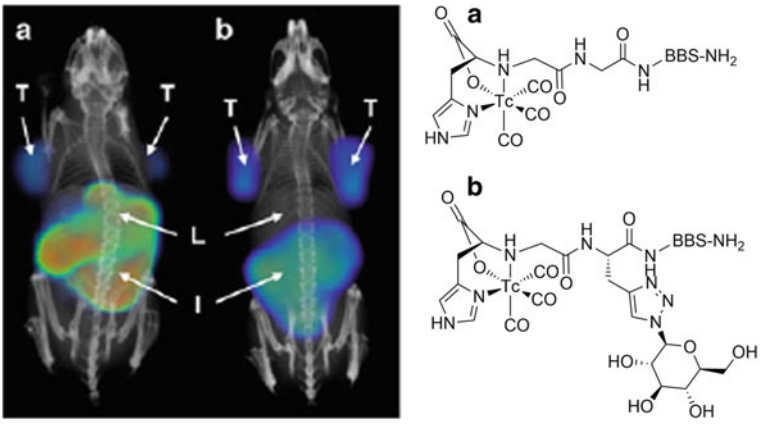

Fig. 7.6 SPECT/CT images of PC-3 tumor-bearing mice 1.5 h after injection of **a** ^{99m}Tc(CO)$_3$-(N$^{\alpha}$His)Ac-βAla-βAla-[Cha^{13},Nle^{14}]BBS(7–14)-NH$_2$ (control compound) and **b** ^{99m}Tc(CO)$_3$-(N$^{\alpha}$His)Ac-Ala(^{N}TG)-βAla-βAla-[Cha^{13},Nle^{14}]BBS(7–14)-NH$_2$, (^{N}TG = N-linked triazole-linked glucose). T = tumor, L = liver, I = intestines [251]

On the other hand accumulation in the liver was significantly reduced. Despite the higher kidney uptake found for the carbohydrated bombesin analogs at early time points after injection, this decreased rapidly with time indicating that the radiotracers were not trapped in the renal tissues. By this example, the strategy of radiotracer glycation has been demonstrated as a potent method to increase the overall hydrophilicity of a tracer and thus to improve the tissue distribution.

Based on the advantages of using trivalent radiometals for preparation of site-directed diagnostic/therapeutic radiopharmaceuticals [98, 268], interest has been sparked into the synthesis and biological evaluation of trivalent radiometalated bombesin derivatives using radioisotopes such as ^{111}In or ^{177}Lu (Table 7.2) [37, 62, 121, 127, 265]. One such example is the bombesin analog referred to as DOTA-AMBA useful for both diagnostic and therapeutic purposes [119, 146, 168]. Also, a so-called pan-bombesin analog has been designed with the special characteristic of displaying high affinity to all three bombesin receptor subtypes possibly allowing a broader field of application [320].

The majority of research efforts into the design of bombesin-based radiotracers have been performed by using GRP receptor agonists. Such bombesin analogs undergo receptor-mediated endoctytosis enabling residualization of the attached radiometal within the targeted tumor cell. However, ^{99m}Tc-demobesin-1 is a potent antagonist, which clearly exhibited high affinity to the GRP receptor even though significant internalization into PC-3 prostate tumor cells was not observed. This radiotracer allowed imaging of PC-3 tumors in mice with higher tumor-to-background contrast compared to the best available agonist analog [178, 205]. Furthermore, an improved quantification of the beta cell mass after pancreas visualization was accomplished with ^{99m}Tc-demobesin-4 combined with a beta cell

imaging with ^{111}In-exendin-3 in rodents [289]. Thus, endeavors were directed also toward the development of bombesin antagonists. Recently, superior imaging properties of the ^{111}In-radiolabeled bombesin antagonist RM1 over the agonist ^{111}In-DOTA-AMBA have been demonstrated [172]. Whether or not bombesin antagonists are also favorable over agonists for therapeutic purposes remains to be investigated.

Dual receptor-targeted probes based on BBN and RGD-peptides combining an integrin $\alpha_v\beta_3$ and GRPR-targeting peptide were developed, e.g., for breast cancer imaging as alternative to ultra sound [49, 125, 126]. They found that this imaging technic is a useful alternative to US but cannot replace US. Furthermore, a ^{99m}Tc-labeled RGD-BBN peptide was used to image lung carcinoma (Lewis lung carcinoma (LLC), U87MG human glioma, and PC-3 human prostate cancer cells) in a small-animal model. It was possible to detect subcutaneous and pulmonary metastatic Lewis lung carcinomas and to distinguish tumor from inflammation using ^{99m}Tc-RGD-BBN [164]. Other attempts dealt with the connection of shepherdin (79–87) to BBN as an inhibitor of the survivin-Hsp90 interaction and Hsp90 ATPase activity [86]. To use the therapeutic impact, ^{99m}Tc has to be located at the nucleus of the cells. For this purpose, BBN was connected to the TAT (49–57) peptide and radiolabeled with ^{99m}Tc with N_2S_2 as chelating moiety [237]. Cell binding and proliferation were tested showing an efficient internalization to PC-3, MDA-MB231, and MCF7 cells with a significant reduction in the cell proliferation.

7.3.3 Neurotensin Analogs

Neurotensin (NT) is a linear tridecapeptide that can be found in the central nervous system and in peripheral tissues. Among the three NT receptors (NTR), NTR1 has been found in several neuroendocrine tumor types. Of special interest are exocrine pancreatic carcinomas that overexpress NTR1 with an incidence of 75–88% [224]. Thus, several studies focused on the development of NT analogs for radiolabeling with SPECT radionuclides such as ^{99m}Tc [94, 95, 170] and ^{111}In [11, 63]. Similar to other small neuropeptides, neurotensin is rapidly metabolized in plasma by endogenous peptidases. Thus, neurotensin analogs which are stabilized at one or more of the three potential cleavage sites were developed. In this respect, the research group of Maina and Nock developed several ^{99m}Tc(V)-neurotensin analogs, referred to as ^{99m}Tc-demotensin, employing amino acid substitutions and/or reduction in the amide bond Arg^8/Lys^8-Arg^9 to the corresponding amine [170, 207]. Garcia and co-workers reported the biological evaluation of neurotensin analogs in which two of the three cleavage sites have been stabilized [39, 95, 169]. These interventions allowed the preparation of neurotensin analogs of high plasma stability, affinity to the NTR1 in the nanomolar range, and significant tumor uptake in preclinical and clinical studies. A promising candidate is the ^{99m}Tc radiolabeled peptide (N^{α}-His)Ac-Arg-(N-CH_3)-Arg-Pro-Tyr-Tle-Leu (^{99m}Tc-NT-XII), which has been stabilized at the cleavage sites 8–9 and 11–12. Other than in the case of bombesin derivatives (see Sect. 7.3.2), the introduction of a glycomimetic entity

(shikimic acid) coupled to the side chain of an additional lysine residue did not result in an improved tissue distribution of the radiotracer. Although the expected lower kidney and liver uptake could be achieved, both the receptor affinity and the tumor uptake were unfavorably reduced. Recently, the group of Garcia reported the evaluation of a $^{99m}Tc(CO)_3$-neurotensin analog, ^{99m}Tc-NT-XIX, modified at all three cleavage sites [94, 95]. Despite a slight decrease in receptor affinity and a lower rate of internalization, the in vitro and in vivo stability of this novel radiopeptide has been significantly increased (Table 7.3).

This example of a triple-stabilized neurotensin analog demonstrates the importance of the radiotracer's metabolic stability to increase its accumulation in the tumor tissue which was—in the case of ^{99m}Tc-NT-XIX—even able to compensate a slightly lower receptor-binding affinity. The clearly improved tumor-to-background contrast of ^{99m}Tc-NT-XIX over ^{99m}Tc-NT-XII could be visualized by SPECT/CT imaging (Fig. 7.7). Thus, the development of neurotensin ^{99m}Tc-radiotracers, where single-amino acids have been substituted for peptide stabilization, is an example for optimization of a radiotracer's tissue distribution by increasing its in vivo stability.

7.3.4 Other Peptide-Based Radiotracers

Beyond somatostatin and GRP receptor targeting with bombesin and neurotensin analogs, many other regulatory peptide receptors are overexpressed on a variety of tumor types. Thus, peptide analogs in various stages of preclinical or clinical development include derivatives of cholecystokinin-2 (CCK-2) [60], glucagon-like peptide-1 (GLP-1) [138], neuropeptide Y (NPY) [322], and Arg-Gly-Asp (RGD) peptides [246] among others. CCK-2 receptors are expressed in medullary thyroid cancers. Initial gastrin-ligands for CCK-2 receptor targeting comprising a DTPA-DGlu-chelator showed unfavorable tumor-to-kidney ratios of radioactivity accumulation and were therefore not developed further. New gastrin derivatives lacking the glutamate-moiety showed excellent CCK-2 receptor affinity and lower renal retention in a rat AR42J tumor model [103]. Recently, it was found that

Table 7.3 Stability and affinity of different radiolabeled NT analogs [94]

Analog	Amino acid sequence	In vitro stability		In vivo stability	Affinity
		Plasma	HT-29	Blood	K_d (nM)
^{99m}Tc-NT-II	(N^{α}-His) Ac-Arg-Arg-Pro-Tyr-Ile-Leu	5.6 min	n.d.	<1 min	0.3 ± 0.2
^{99m}Tc-NT-XII	(N^{α}-His)Ac-Arg-(**N-CH$_3$**)-Arg-Pro-Tyr-**Tle**-Leu	21 d	6.5 h	0.75 h	2.0 ± 1.6
^{99m}Tc-NT-XIX	(N^{α}-His)Ac-Arg-(**N-CH$_3$**)-Arg-Pro-**Dmt-Tle**-Leu	28 d	2.4 d	1.40 h	15.0 ± 9.2

The modifications in the binding sequence are marked in *bold*
(*N^{α} His*)*Ac* Retro[N^{α}-carboxymethyl-histidine], *Tle* tertiary-leucine, *Dmt* dimethyltyrosine, *n.d.* not determined

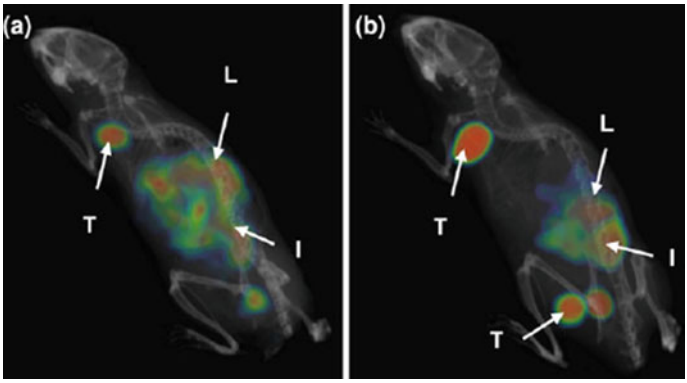

Fig. 7.7 SPECT/CT images of HT-29 tumor-bearing mice 1.5 h after injection of **a** ^{99m}Tc-NT-XII and **b** ^{99m}Tc-NT-XIX. T = tumor, L = liver, I = intestines [94]

GLP-1 receptors are highly overexpressed in virtually all insulinomas and gastrinomas [138]. Metabolically more stable GLP-1 congeners referred to as exendin-3 and exendin-4 have been derivatized with a DTPA or DOTA chelating system for radiolabeling with ^{111}In or lanthanide radioisotopes. Remarkable tumor targeting was found in a human patient while employing ^{111}In-DOTA-exendin-4 [51]. NPY analogs are of interest because of the frequent overexpression of NPY receptors in a variety of tumor types including breast cancer. A recent article reports on the synthesis and evaluation of a large number of NPY analogs where a DOTA-derivatized compound radiolabeled with ^{111}In performed as a potent radiotracer [322]. However, the in vivo studies with this tracer showed only a low tumor uptake whereas radioactivity retention in the kidneys was extremely high. RGD peptides that do not belong to the group of regulatory peptides are of particular interest for targeting integrin receptors such as the $\alpha_v\beta_3$ integrin. This integrin subtype is strongly expressed on activated and proliferating endothelial cells during tumor angiogenesis and metastasis but is not readily detectable in resting endothelial cells and most normal organs. Thus, a variety of RGD-peptide analogs for targeting $\alpha_v\beta_3$ integrins have been developed and the promising potential of RGD-based radiotracers for SPECT radio imaging has been shown [246]. To enhance binding affinity for the $\alpha_v\beta_3$ integrin, various multivalent cyclic RGD-based peptides have been developed. All oligomeric peptide probes bound more strongly to the target cells than the monomeric RGD peptide in an integrin $\alpha_v\beta_3$-positive U87MG xenograft mouse model (Fig. 7.8) [260, 299].

Through RGD peptides the advantage of multivalent tumor-targeting agents over monovalent agents has been demonstrated. Most likely, the employment of the multimer-strategy also improves tumor-targeting properties of non-RGD-based peptides. Accordingly, investigations of divalent and multivalent peptides are ongoing for targeting of many of the tumor-associated receptors mentioned above, among those imaging agents for targeting the CCK-2 receptor [271] and somatostatin

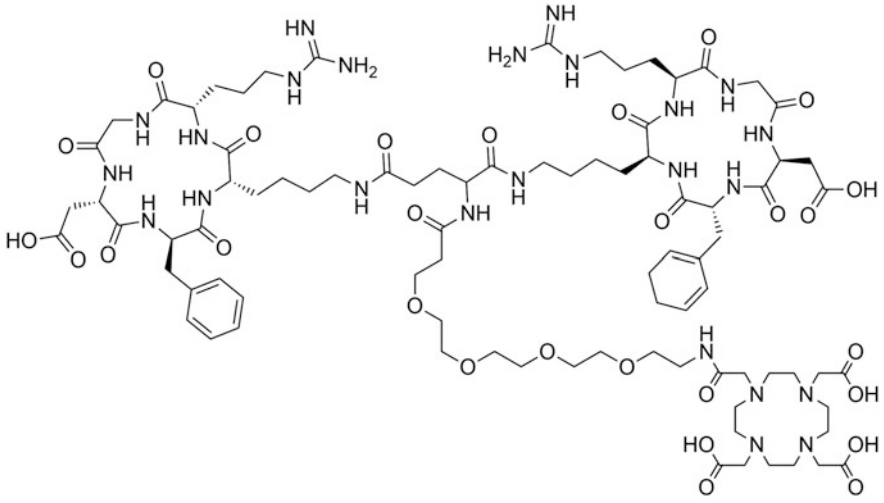

Fig. 7.8 Chemical structure of DOTA-3PEG$_4$-RGD dimer [158, 259]

receptor [312]. Also, the strategy of using dual tumor-targeting agents that combine targeting ligands for two different receptors (e.g., integrin and GRP receptor) might improve the radiotracer's diagnostic utility and applicability [162, 163].

7.4 Antibodies and Antibody Fragments

Another approach of nuclear imaging is the use of radiolabeled antibodies that target-specific cell surface antigens. Radioimmunoimaging has been traditionally developed in parallel with radioimmunotherapy for the evaluation of the antibodies' targeting properties and for dosimetry. Common tumor-associated targets for radioimmunoimaging (and -therapy) are epidermal growth factor receptors (EGFR) [281, 309], the carcinoembryonic antigen (CEA) [123], the prostate-specific membrane antigen (PSMA) [152], cluster of differentiation antigens (e.g., CD20), the pancarcinoma antigen (TAG-72), and the HER2 receptor among others. In addition, a number of angiogenesis markers—protein antigens expressed either on blood vessels or in the adjacent matrix of vessels—have been characterized as targets for selective delivery of antibodies to the tumor neovasculature [36]. Examples are the fibronectin extra-domain B (EDB) [204], the integrin $\alpha_v\beta_3$ [217], the vascular endothelial growth factor (VEGF) [38], and annexin A1 [209].

Potential concerns for radioimmunodiagnosis and strategies for optimization have been summarized in several review articles [41, 42, 293]. The main disadvantage of antibodies, namely their immunogenicity, could be largely overcome by the application of humanized antibodies that evade the immune system and are

resistant to degradation. However, the slow vascular clearance (days to weeks) of antibodies as a consequence of their high-molecular-weight (IgG antibodies: ~150 kDa) and the low tissue penetration are generally disadvantageous for radioimaging because of the resulting low target-to-non-target contrast at early time points after administration. Although it is generally accepted that antibodies are not the preferred biomolecules for nuclear imaging, the application of antibody fragments for SPECT has been successfully exemplified. Similar to peptides, antibody fragments are rapidly cleared from the blood and from non-targeted tissues. The results thereof are higher tumor-to-background ratios compared with intact antibodies and a lower radiation absorbed dose in non-targeted tissues and organs. A reduced percentage of injected doses of radioactivity in the tumor tissue and higher radiation doses in the kidneys are also consequences of the reduced size of antibody fragments [42].

Efforts have been directed toward the development of antibody fragments such as $F(ab')_2$, F(ab′) and single-chain Fv (scFv) fragments to achieve faster clearance from the blood and in addition a better tumor penetration [313, 314]. Application of high-affinity scFv resulted in a relatively high tumor uptake combined with a rapid blood clearance and hence favorable targeting ratios [27]. Multimers of antibody fragments may result in improved tumor localization compared with monomeric species as a result of higher affinity and slower blood clearance [134].

Another approach to achieve improved pharmacokinetics is the pretargeting strategy. Pretargeting involves an initial targeting agent, which itself can be bound by secondarily injected agents. Secondary agents are either quickly clearing radiotracers that bind the initial agent with high affinity [102, 151, 213, 249, 273] or "chase" reagents that clear an unbound radiolabeled antibody in circulation [135]. The pretargeting approach is, however, not commonly applied for SPECT. In contrast, this strategy is much more favorable for radioimmunotherapy in order to reduce the radioactive dose burden to the bone marrow and thus to avoid potential hemotoxicity of long circulating antibodies labeled with particle-emitting radioisotopes.

Radioimmunoimaging is of particular interest to evaluate a potential application of antibodies for targeted radionuclide therapy by interchanging a diagnostic with a therapeutic radioisotope of similar chemical characteristics (e.g., ^{111}In and ^{90}Y) or using a therapeutic radionuclide that emits concomitantly with therapeutic radiation also diagnostic γ-rays of a suitable energy for SPECT (e.g., ^{177}Lu, Table 7.1). The most prominent example of an antibody employed for radioimmunotherapy is ibritumomab tiuextan (Zevalin), a ^{90}Y-radiolabled monoclonal anti-CD20 antibody for the treatment of non-Hodgkins lymphoma. Its ^{111}In-radiolabeled counterpart is usually administrated prior to therapy for detection of receptor-positive malignant tissue via SPECT imaging and for dosimetry.

7.4.1 Targeting Fibronectin Extra-Domain B: Antiangiogenic Antibody Fragment L19

Angiogenesis is an underlying process in many human diseases, including cancer. An established target in this respect is the extra-domain B of fibronectin (EDB), a domain of 91 amino acids, which is typically inserted in fibronectin molecules at sites of tissue remodeling but not in fibronectin molecules under normal conditions. Thus, the expression of EDB has been shown in malignant tumors but not in healthy tissues [315]. The Neri group has isolated a number of human monoclonal antibodies to EDB [43, 204, 215]. The human antibody fragment, scFv(L19) displayed subnanomolar affinity to EDB and has been shown to efficiently localize on tumoral neovasculature in animal models [68]. Importantly, the ^{123}I-labeled dimeric L19 antibody fragment L19(scFv)$_2$ has been evaluated for targeting primary tumors and metastatic lesions in cancer patients through immunoscintigraphy [236]. This clinical study was performed with 20 patients whereof the majority had colorectal or lung cancer. It could be demonstrated that the antibody ^{123}I-L19(scFv)$_2$ selectively accumulated in malignancies and allowed distinguishing among actively growing and quiescent lesions. Another Phase I/II clinical immunoscintigraphy study used ^{123}I-L19(scFv)$_2$ in patients with head and neck squamous cell carcinoma [32]. It was observed that for head and neck scintigraphy, iodinated antibodies have severe disadvantages. Although the thyroid gland was protected by competitive application of non-radiactive iodide, there were substantial artifacts in this area in all cases as a result of the uptake of liberated free iodide that was always present to a certain degree. Since dehalogenases are present in the salivary glands, free iodide also gave a high background in the 4 h postinjection scintigraphy in the parotid and submandibular glands as well as in the minor salivary glands of the oral and nasal mucosa. Although the ^{123}I-L19(scFv)$_2$ is probably less suited as a diagnostic imaging modality for head and neck cancer, L19(scFv)$_2$ offers a general potential to be used as a tumor-targeting agent for both diagnostic and therapeutic purposes. Because neovasculature and tissue remodeling are required for the growth of all aggressive solid tumors, imaging approaches that use angiogenesis markers can be used for different types of cancer. An advantage of this strategy might be the fact that noninvasive imaging of angiogenesis via EDB fibronectin targeting allows the discrimination between quiescent and actively growing lesions.

7.5 Vitamin-Based Radiotracers

The use of small-molecular-weight targeting compounds is favorable to surmount the drawbacks of long circulation times and thus poor tumor-to-background contrast as well as possible immunogenicity encountered with antibodies. In this respect the application of vitamins as targeting agents provides several advantages: vitamins are small in size, inexpensive, relatively easily amenable for chemical modification, and non-immunogenic. Rapidly dividing cancer cells have an

increased demand for certain vitamins such as folates, vitamin B12 (cobalamin), biotin, and riboflavin. These B-group vitamins are required for cell survival and proliferation because they act as co-enzymes of biochemical reactions that are essential for the synthesis of amino acids and for nucleotide bases [233]. The most thoroughly investigated vitamin to be used as tumor-targeting agent is folic acid. The utility of folic acid conjugates has been widely exemplified in a variety of (pre)clinical studies for targeting the folate receptor (FR) that is overexpressed on a wide variety of cancer types [165]. Also, it has been demonstrated that vitamin B_{12} has the potential to be used as cancer-targeting agent whereas only few studies have focused on the applicability of biotin for direct tumor targeting [233]. Since vitamins are indispensable for sustaining life, it is unlikely that a mutational arrest of vitamin uptake would occur with concomitant failure of vitamin-mediated diagnosis or therapy. This is a distinct feature of vitamins and an advantage for their application as tumor-targeting agents. Thus, using vitamin-based imaging agents is attractive and the strategy holds promise to also be used for therapeutic purposes.

7.5.1 Folic Acid Conjugates

Folic acid and folates (reduced forms) are water-soluble vitamins of the B-complex group. Humans cannot synthesize folates and hence must necessarily obtain them from food. Although only small quantities of folates are required, these vitamins are vital for various biochemical reactions including those for the synthesis of RNA and DNA, amino acid metabolism, and gene regulation. Cellular uptake of folates is accomplished by either carrier systems or the high-affinity folate receptor (FR). The FR is a glucosylphosphatidylinositol (GPI)-anchored protein that is frequently overexpressed in a variety of tumor types including cancers of the breast, ovaries, cervix, endometrium, lungs, kidneys, colon, and brain [13, 212]. In normal organs and tissues, FR-expression is highly restricted to only a few sites where it is located on the apical side of polarized epithelia in the lung, the placenta, and the choroid plexus of the brain and in the proximal tubule cells of the kidneys [13, 212, 304]. Thus, folic acid can be used as a molecular "Trojan horse" for selective delivery of attached probes to FR-positive cancer cells [165]. During the last decades, a variety of folic acid conjugates of radioisotopes useful not only for SPECT imaging (^{99m}Tc, ^{111}In, ^{67}Ga) has been developed and evaluated (Fig. 7.9) [16, 79, 130, 131, 196–198, 264]. Biodistribution studies of radiofolates in mice showed a specific uptake in FR-positive tumor (xeno)grafts, whereas unspecific radioactivity in background tissues was rapidly cleared in particular if the derivatives displayed hydrophilic properties. In the kidneys, however, high radioactivity retention was observed as a consequence of the specific binding of radiofolates to FRs expressed in the proximal tubule cells. This process results in unfavorably low tumor-to-kidney ratios of radiofolates in general. Clinical application of the two most promising candidates, ^{111}In-DTPA-folate [179, 261, 300] and ^{99m}Tc-EC20 [87, 149, 223], also known as ^{99m}Tc-etarfolatide or FolateScan, revealed the same phenomenon in humans that was previously found in tumor-bearing mice [181]. ^{99m}Tc-EC20 is currently

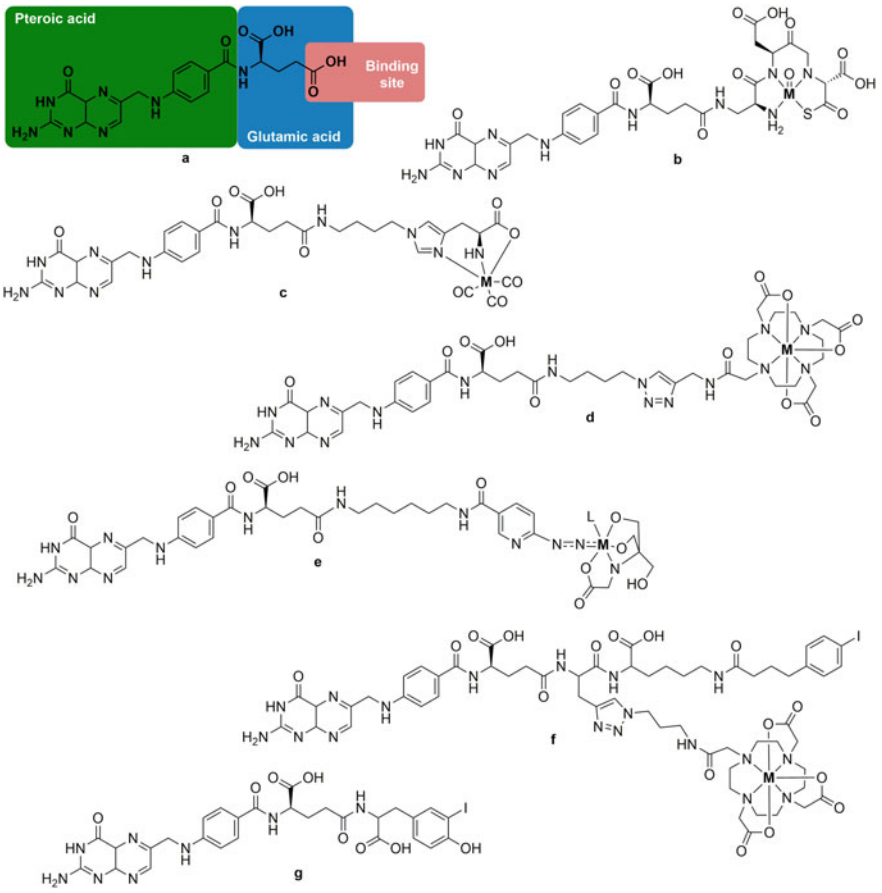

Fig. 7.9 Chemical Structures of the vitamin folic acid. **a** EC20 (M = ^{99m}Tc). **b** His-folate (M = ^{99m}Tc, ^{188}Re). **c** DOTA-folate (M = ^{111}In, ^{177}Lu). **d** ^{99m}Tc-HYNIC-folate. **e** DOTA-folate with albumin-binding entity (M = ^{161}Tb, ^{177}Lu) **f** and ^{125}I-folate (**g**)

undergoing Phase 1 and 2 clinical trials in several institutions within the US and Europe. Mostly, renal cell carcinomas, pituitary adenomas, ovarian, and breast carcinomas were investigated. While imaging of malignant tissue could be successfully achieved, high radioactivity uptake was found in the kidneys of patients where the FR is expressed to approximately the same level as in mouse kidneys [212]. Healthy volunteers were enrolled in another phase I clinical study to assess the pharmacokinetics in terms of safety and radiation dosimetry. The activity of ^{99m}Tc-EC20 at 5 min postinjection was largest in the bone marrow, followed by the liver and kidneys, and decreased in all organs/tissues within 1 day without appreciable retention [310]. In a phase II multicenter study, 43 patients with advanced ovarian cancer were imaged with ^{99m}Tc-EC20 for lesion detection before

treatment with vintafolide [189]. In a 2009-reported clinical study, ^{99m}Tc-EC20 was used to determine inflammatory diseases like rheumatoid arthritis in comparison with healthy humans. It could be illustrated that imaging with ^{99m}Tc-EC20 is more sensitive for these diseases compared to physical examinations [180].

In an attempt to improve the low tumor-to-kidney ratio of radiofolates, it was hypothesized that application of antifolates (e.g., pemetrexed) could increase the "appetite" of the tumor cells for folates and thus lead to an increased accumulation of folic acid conjugates. This hypothesis was confirmed in vitro [190]. However, in mice that were treated with antifolates, radiofolate uptake in tumor xenografts was not increased. While approaching this hypothesis, injection of pemetrexed was accomplished at different time points prior to the radiotracer. None of the experiments revealed an increased tumor accumulation of radioactivity, however, surprisingly administration of pemetrexed short before the radiofolate resulted in a significant reduction in kidney uptake [190]. The result was a tremendous increase in the tumor-to-kidney ratio of radioactivity. This effect could be reproduced with a variety of folic acid conjugates radiolabeled with various radionuclides (^{99m}Tc, ^{188}Re, ^{111}In, ^{125}I, ^{146}Tb, ^{177}Lu) and in mouse models bearing different tumor (xeno)grafts (KB, IGROV-1, SKOV-3; M109) [191–193, 195, 199–201, 222]. The clearly superior SPECT imaging quality of mice that received pre-dosed pemetrexed could be impressively demonstrated while using ^{111}In-radiolabeled DTPA-folate (Fig. 7.10). This example demonstrates a pharmacological intervention by a non-radioactive substance that results in an improved tissue distribution of the radiotracer compared to the results obtained after radiotracer administration alone.

Another approach to reduce the kidney uptake deals with the modification of the backbone of the folate conjugate. For this purpose, an albumin-binding entity was connected to enhance the circulaton time of the radioconjugate in the blood associated with an increase in the tumor-to-kidney ratio. In this regard, other radionuclides for imaging (^{44}Sc, ^{64}Cu, and ^{68}Ga for PET) and therapy (^{177}Lu, ^{47}Sc) were applied to survey the therapeutic eligibility [78, 197, 200, 264]. Other approaches dealing with the combination of bombesin (1–14) with a DOTA-FA as theragnostic

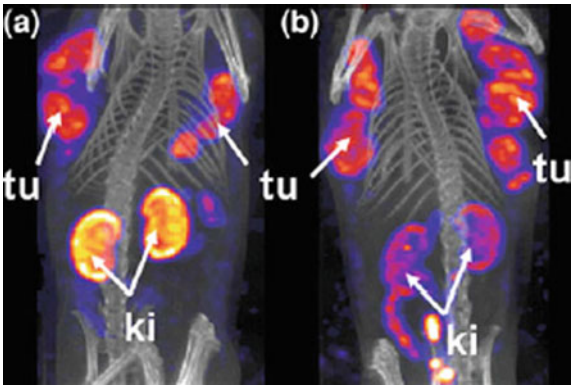

Fig. 7.10 SPECT/CT of mice injected with **a** ^{111}In-DTPA-folate only and **b** in combination with pre-dosed pemetrexed

agent labeled with ^{177}Lu for breast cancer showed a higher tumor uptake as the DOTA-FA alone in T47D-tumor-bearing mice combined with a high renal clearance [14]. HYNIC is known to bind Tc efficiently. Thus, approaches with FA-HYNIC conjugates [167] using a click chemistry approach for the linkage of the Tc-core and FA [108] and a multimerization of FA [109] were presented. However, the best tumor-to-organ ratio was found with the PEGylated monomer using KB tumor-bearing mice. Nanocarriers like PAMAM were extensively studied as well. A PAMAM-DTPA-conjugate was presented showing a high tumor accumulation (13.34%ID) combined with an uptake in the liver (9.48%ID) and the heart (6.88%ID/g) after 3 h pi in KB-bearing mice [321]. The PAMAM-HYNIC-conjugate showed a substantial accumulation in the tumor (10.61%ID/g), but the uptake in liver with 69.34%ID/g and spleen with 14.43%ID/g combined with a blood content of 7.68%ID/g was high after 3 h pi in BALB/c mice with 4T1-breast cancer [203]. Other nanocarriers based on poly(ethylene glycol)-poly(lactic-co-glycolic acid) were used with a particle size of 104–128 nm mean showing a high tumor uptake (21.3%ID/g), but also a high uptake in liver, kidneys, spleen, and blood of > 13%ID after 3 h pi in SKOV-3-bearing tumor mice. Efforts to develop nanoprobes as ^{99m}Tc-imaging agents were made by the use of nanographene oxide (nGO). Thus, nGO was modified with PEG and further functionalized with FA ready for labeling with $^{99m}TcO_4^-$ and $SnCl_2$. A biodistribution study using mice demonstrated a long residence time in the blood; a high accumulation in liver, spleen, lung, and kidneys; and a comparatively low uptake in the tumor [77].

Humanized IgG1 antibodies like farletuzumab that specifically recognizes the folate receptor alpha (FRα) were radiolabeled with ^{111}In and additionally with a fluorescent dye to use this radiopharmaceutical for the intraoperative detection of ovarian cancer lesions. ^{111}In-farletuzumab-IRDye800CW showed optimal tumor-to-blood ratios of 3.4–3.7 at protein doses up to 30 μg in mice with intraperitoneal IGROV-1 tumors and can be blocked by coinjection of an excess of unlabeled farletuzumab [113].

7.5.2 Vitamin B_{12} Conjugates

The earliest studies of radiolabeled vitamin B_{12} (cobalamin) using cobalt radioisotopes (^{57}Co, ^{58}Co, ^{60}Co) showed radioactivity accumulation in peripheral, actively growing tumors with highest accumulation in sarcomas [33, 88, 89]. Other studies used radioiodinated arylstannylcobalamin conjugates showing enhanced uptake into renal carcinomas in nude mice when compared with other healthy tissues and organs [307]. Collins et al. developed ^{111}In-DTPA-analogs of cobalamin (DTPA cobalamin analogs = DACs) and tested them in preliminary biodistribution experiments in mice with CCL8 sarcomas and in pigs [53]. The overall biodistribution of DACs showed tumor uptake and high radioactivity accumulation in healthy organs that were almost identical to previous studies performed with $^{57/60}$Co-radiolabeled vitamin B_{12}. The same group reported the first patient study performed with ^{111}In-DTPA-adenosylcobalamin for cancer imaging [54].

^{111}In-DTPA-adenosylcobalamin was found to be effective for detection of high-grade aggressive tumors in humans with the most successful results in patients with breast cancer and high-grade lung, colon, thyroid, and sarcomatous malignancies [55]. However, the most significant uptake of these cobalamin derivatives was found in the liver, kidneys, and spleen followed by radioactivity accumulation in several glands. Vitamin B_{12} is bound to soluble transport proteins in circulation, namely, transcobalamin I (TCI), intrinsic factor (IF), and transcobalamin II (TCII) whereof the latter is the principle vitamin B_{12} binding protein [252–254]. TCII-cobalamin binds to TCII-receptors that are ubiquitously expressed in cells for effective acquisition of this important vitamin. Originally, vitamin B_{12}-mediated tumor targeting was thought to be dependent on undisturbed interaction of cobalamin with these main transport systems and tumor uptake were believed to be mediated via up-regulated TCII-receptors [25, 233]. Later, it was hypothesized that selective TCII non-binders would lead to improved tissue distribution. Various cobalamin derivatives comprising a (pyridine-2-ylmethylamino)acetic acid (PAMA) chelator for coordination of the ^{99m}Tc-tricarbonyl core were developed with different spacer lengths [C-2 to C-6, i.e., $(-CH_2-)_n$, n = 2–6]. $^{99m}Tc(CO)_3$-PAMA-cobalamin derivatives with a spacer length of C-5 or longer displayed TCII binding affinity whereas those with shorter spacer lengths (C-2 to C-4, Fig. 7.11) were identified as TCII non-binders, but displayed retained interaction with IF and TCI [298]. The results of biodistribution studies in tumor-bearing mice performed

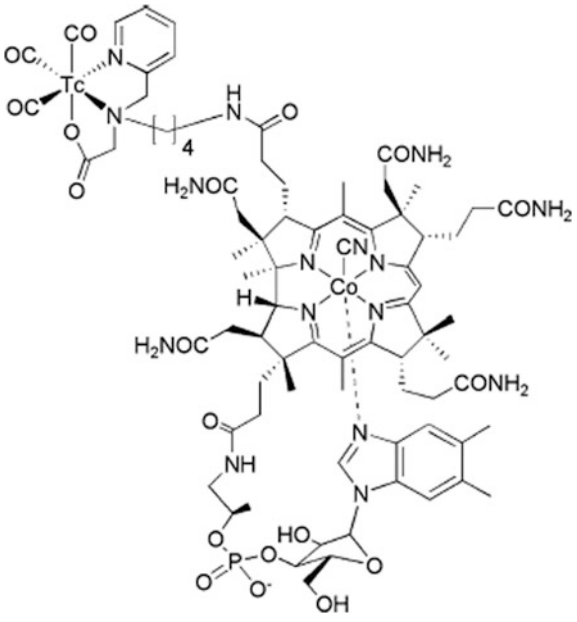

Fig. 7.11 Chemical Structure of ^{99m}Tc-PAMA-C4-cobalamin, a TCII non-binder vitamin B_{12} derivative

with ^{99m}Tc(CO)$_3$-PAMA-C5-cobalamin and ^{99m}Tc(CO)$_3$-PAMA-C6-cobalamin were similar to previously evaluated ^{111}In-DTPA-adenosylcobalamin tracers [298]. In contrast, data of ^{99m}Tc(CO)$_3$-PAMA-cobalamin derivatives with spacer lengths shorter than C-5 showed a significantly improved tumor-to-blood and tumor-to-kidney ratio of radioactivity. Thus, abolished interaction of the radiolabeled cobalamin tracer with TCII resulted in decreased accumulation of the radiotracer in the blood and in organs and tissues that would otherwise be predestined to have high cobalamin uptake such as kidneys and diverse glands (Fig. 7.12).

^{99m}Tc(CO)$_3$-PAMA-C4-cobalamin (Fig. 7.11) was selected as the most favorable candidate because it displayed the highest tumor-to-blood and tumor-to-kidney ratios in animal experiments. These findings suggest that the transport of cobalamin derivatives into malignant tissue is not dependent on the transport protein TCII but rather mediated via TCI. By this example, it could be demonstrated that variation of the radiotracer's linker length could have a tremendous impact on the overall tissue distribution of a radiotracer and thus, on its successful application. Excellent results achieved in preclinical studies paved the path toward a clinical application of cobalamin-targeted radioimaging in patients using the TCI-selective organometallic ^{99m}Tc-vitamin B$_{12}$ derivative.

7.5.3 Other Vitamin Targeting Agents—Pretargeting

It is likely that carriers and receptors of vitamins other than folates and vitamin B$_{12}$ could be used for tumor-targeted nuclear imaging purposes. Among the vitamins of the B-group, it was suggested that cancer cells also overexpress a biotin receptor that could, however, not yet be identified [186, 233, 311]. Additionally, a possible reason for the generally little interest in biotin as a direct tumor-targeting agent could be the fact that renal filtration and reabsorption of biotin and its conjugates

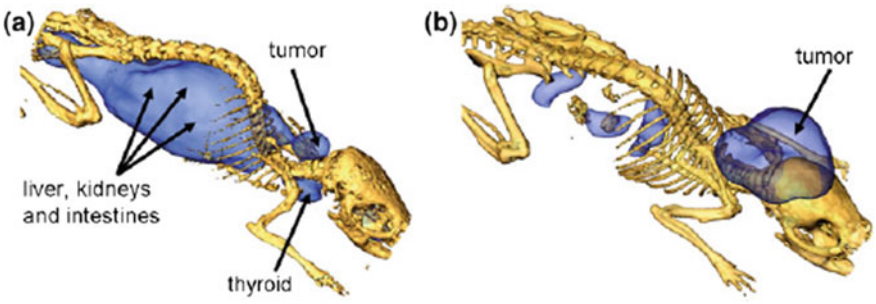

Fig. 7.12 Whole-body SPECT/CT scans of B16F10 tumor-bearing mice, 24 h after injection of **a** ^{99m}Tc(CO)$_3$-PAMA-C6-cobalamin (TCII binder) and **b** ^{99m}Tc(CO)$_3$-PAMA-C4-cobalamin (TCII non-binder)

lead to high renal uptake of radioactivity in the kidneys. Recently, it was shown that vitamin C (ascorbate) conjugated nanoparticles could be delivered into the brain presumably via the sodium-dependent ascorbic acid transporter SVCT2 whose RNA was found in the choroid plexus epithelium [234]. The SVCT2 carrier was found on rat glioma cells (C6 and F98) and on mouse fibroblasts (NIH/3T3). This study introduced the perspective of using the SVCT2 transporter for brain targeting through the choroid plexus where it is selectively expressed. There might also be a potential to use this vitamin C transporter for nuclear imaging purposes of cancer diseases in the future.

Efforts have been done to use biotin as component in the (strept)avidin–biotin-pretargeting system as their strong affinities ($K_d = 10^{-15}$ M) allow the in vivo radiolabeling of high-molecular-weight compounds like proteins, antibody fragments, or antibodies for imaging and radiotherapy [257]. The problems of slow distribution kinetics of these compounds in association with insufficient tumor-to-organ ratios combined with a slow blood clearance should be avoided with this system in contrast to the application of directly radiolabeled biomacromolecules. For this purpose, the biomacromolecule (e.g., antibody) was connected to the (strept)avidin and the radionuclide was connected to the biotin or in the opposite way (Fig. 7.13).

In general, the pretargeting system consists of three steps [35]. First, a non-radiolabeled but avidin-functionalized antibody was administered intravenously allowing a slow distribution and the binding to the target site over 2 to 3 days in vivo. Afterward in the second step, a clearing agent was given that helps to remove the remaining unbound antibody from the body whereas the antibody reaches the highest uptake in the targeted tissue. In the third step, a radiolabeled conjugate was administered, which consists of the biotin bearing the radiolabel. This radioconjugate binds with a high affinity to the (strept)avidin-functionalized antibody given previously and exhibits fast distribution properties in vivo. Due to the fast blood clearance of the biotin-radioconjugate through the kidneys, a high tumor-to-background ration will be achieved combined with a protection of the liver. Importantly, the antibody itself has to be located at the surface of the cell during the time of the radioconjugate injection. It should not be internalized.

The first approach to use the avidin–biotin-system for radiolabeling purposes was accomplished by Hnatowich and co-workers [118]. A biotin-conjugated antibody and a DTPA-coupled avidin were used and the radiolabeling was done with ^{111}In. They showed that the target/non-target radioactivity ratios were significantly improved with respect to the conventional radiolabeling procedures. Later, Rosebrough discovered the pharmacokinetics and biodistribution of radiolabeled avidin, streptavidin, and biotin [231] using rabbits and dogs. He found that both ^{111}In-DTPA-biotin and ^{111}In-DTPA-biotin–avidin have a high excretion rate (<5% circulation in the blood after 1 h) in contrast to the ^{111}In-labeled DTPA-biotin–streptavidin-conjugate (>30% after 6 h). In this regard, ~80% of the dose of ^{111}In-DTPA-biotin–avidin was found in the liver after 6 h. In contrast,

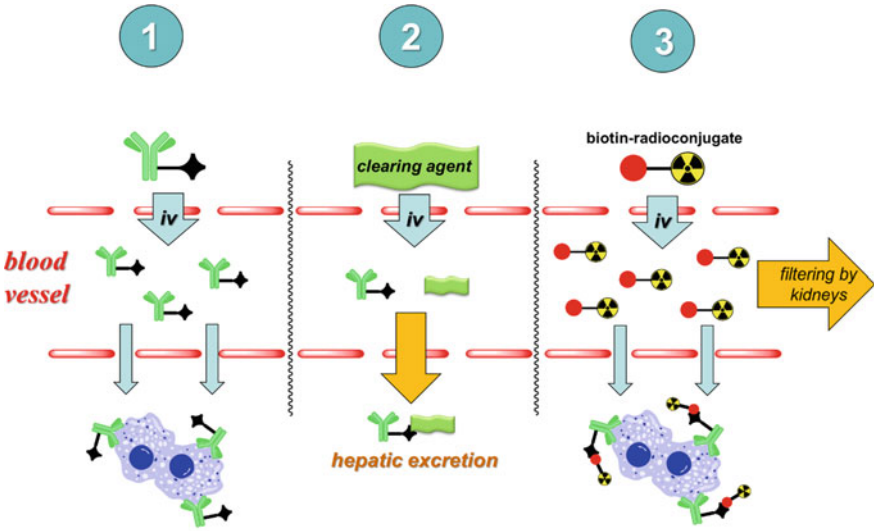

Fig. 7.13 Pretargeting concept using a radiolabeled biotin-conjugate and a (strept) avidin-functionalized antibody. Step 1: distribution of the functionalized antibody to the target (tumor cells); Step 2: clearance of the unbound antibody from the blood; Step 3: administration of the biotin-radioconjugate and binding to the antibody (remaining biotin-radioconjugate will be excreted rapidly)

^{111}In-DTPA-biotin–streptavidin had only ~5% liver accumulation 6 h after injection. They and others stated that the blood clearance of the radiolabeled streptavidin and avidin differed markedly due to the difference in net charge exhibited at physiological pH [124]. Based on these facts, attempts were done to decrease the uptake of streptavidin in the liver [110, 308].

A multitude of biotin–chelator-conjugates not only for ^{99m}Tc [136, 148] but also for ^{111}In [18] and ^{68}Ga [280] or dual modality imaging probes [70] as well as for pretargeted radioimmunotherapy with ^{90}Y, ^{67}Ga, ^{177}Lu, and other therapeutic radionuclides were developed [155, 183]. Additionally, biotin conjugates for biorthogonal click chemistry were designed (see, e.g., [139, 218]); examples are shown in Fig. 7.14. A phase II study with 25 patients bearing a metastatic colon cancer using ^{90}Y-DOTA-biotin-conjugate and a NR-LU-10 antibody/streptavidin-conjugate showed relatively disappointing results in terms of therapeutic efficacy and toxicity, but beneficial information was obtained concerning normal tissue tolerance to low-dose-rate irradiation [140]. A deeper insight to the pretargeting concept in general is published by Liu [156].

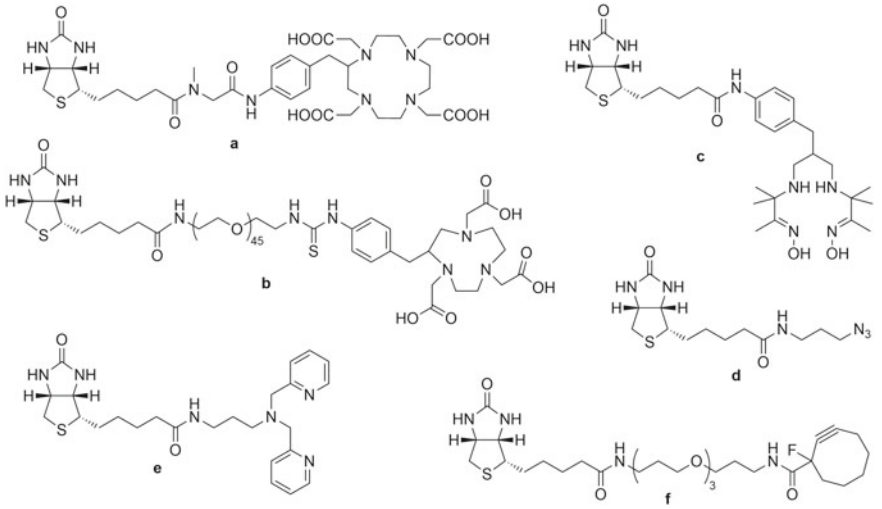

Fig. 7.14 Selected radioconjugates with biotin skeleton containing chelating systems based on macrocycles (**a**) and (**b**); for ^{99m}Tc-labeling (**c**) and (**d**); for bioorthogonal click reactions (**e**) and (**f**)

7.6 Intracellular Targets

7.6.1 ^{99m}Tc-Carbohydrate Complexes

The most frequently used radiotracer for nuclear imaging purposes is currently the glucose analog 2-[^{18}F]fluorodeoxy glucose ([^{18}F]FDG). This PET tracer is taken up by tumor cells mainly by facile diffusion through the glucose transport protein 1 (Glut1). In the cell interior [^{18}F]FDG is phosphorylated by the enzyme hexokinase yielding [^{18}F]FDG-6-phophate which cannot escape the cell anymore. Thus, this trapping mechanism results in accumulation of radioactivity in metabolically active (cancer) cells [270]. The clinical relevance of [^{18}F]FDG promoted the development of inexpensive and readily available ^{99m}Tc-labeled glucose analogs.

Most of the derivatives reported in the literature were ^{99m}Tc(V)-glucose complexes [56, 58, 154, 210, 227, 282, 301, 319]. However, these ^{99m}Tc-tracers did not match the criteria and features of [^{18}F]FDG, such as active transport via Glut1 and phosphorylation via hexokinase. Later, Dapueto and colleagues could show a higher uptake of ^{99m}Tc-IDAG and ^{99m}Tc-AADG into the tumor of melanoma bearing C57BL/6 mice with tumor-to-muscle ratios of 12.1 ± 3.73 and 2.88 ± 1.40 [57].

Endeavors have been undertaken by the group of Schibli and others to design organometallic glucose and glucosamine analogs using the matched pair ^{99m}Tc/$^{186/188}$Re [26, 71, 214, 239]. Later, Lin et al., Zeltchan et al. and Khan et al. reported new ^{99m}Tc-labeled glucose derivatives bearing a ^{99m}Tc(CO)$_3$ core [132,

318]. Both tracers were subjected to cell studies either with Chinese hamster ovary cells CHO, human breast adenocarcinoma MCF-7 cells, and murine sarcoma S180 cells. Following animal studies revealed a substantial uptake into the tumor tissue, but also in excretion organs like liver and kidneys. In addition, the ^{99m}Tc-thioglucose derivative prepared by Zeltchan et al. accumulates in the brain.

Biological characterization has been reported from a variety of organometallic ^{99m}Tc(CO)$_3$-glucose complexes, derivatized at the C-1, C-2, C-3, and C-6 positions with various chelating systems. These compounds were tested for their ability to be internalized into Glut1 expressing cancer cells, HT29, and in addition, it was investigated on whether or not they would be phosphorylated via the hexokinase reaction. Unfortunately, all of the complexes tested appeared not to be recognized and transported via Glut1. The authors stated the likeliness of ^{99m}Tc(CO)$_3$-glucose complexes being sterically too demanding for recognition at the extracellular binding site and/or transportation via Glut1. Also, other than [^{18}F]FDG, the organometallic glucose derivatives were not phosphorylated by hexokinase. Orvig and his collaborators reported several new approaches of organometallic carbohydrate complexes. Among others, they synthesized *N*-hydroxybenzylamino-deoxyglucose derivatives (Fig. 7.15) and carbohydrate-appended hydroxypyridinone derivatives [26, 80–82, 275]. However, most of these compounds revealed neither to be hexokinase substrates nor inhibitors. Although basic cell data of these carbohydrate radiometal complexes is lacking, it is likely that they are not taken up via the Glut1 transporter or other specific transport mechanisms and thus would fail to accumulate in cancer cells in vivo.

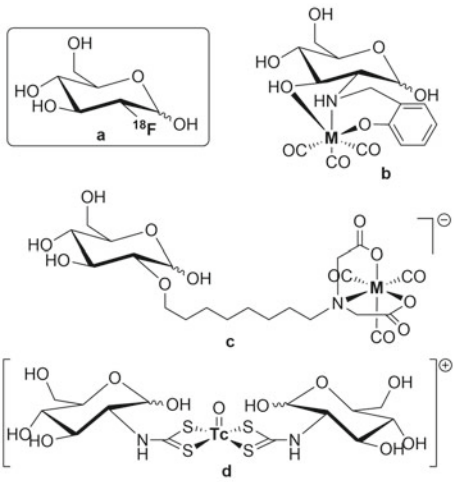

Fig. 7.15 [^{18}F]FDG **a** two C-2 functionalized glucose derivatives of a *N*-(2′-hydroxybenzyl)-amino-chelating system [26] **b** and an imino diacetic acid chelator [239] **c** radiolabeled with ^{99m}Tc-tricarbonyl (M = ^{99m}Tc) and a ^{99m}Tc-tracer based on deoxyglucose dithiocarbamate **d** [154]

7.6.2 Radiolabeled Nucleoside Analogs for Targeting Human Thymidine Kinase

In mammalian cells, salvage pathway phosphorylation of thymidine is catalyzed by two different thymidine kinases (TK): the cell-cycle regulated cytoplasmic TK1 and the constitutively expressed mitochondrial TK2. The human TK1 (hTK1) activity is known to fluctuate with cellular DNA synthesis, the activity being high in proliferating and malignant cells and low or absent in quiescent cells, whereas TK2 activity is low in both dividing and quiescent cells [202]. Since the activity of hTK1 is often dramatically increased in cancer cells, interest has been sparked in targeting this enzyme by radioactive thymidine analogs for selective imaging of proliferating cancer cells. In the cell interior nucleosides are rapidly phosphorylated to nucleotides, which renders them unable to penetrate biological membranes and thus they are "trapped" inside the cells. Thymidine and thymidine analogs labeled with PET radioisotopes such as [^{11}C]methyl-thymidine, 5-[^{76}Br]bromo-2′-fluoro-2′-deoxyuridine, and 3′-[^{18}F]fluoro-3′-deoxythymidine ([^{18}F]FLT) are either under development or already in use as proliferation marker [40, 96]. However, due to the high costs for the production of PET radioisotopes and the unfavorably short half-lives of PET isotopes, the use of SPECT radioisotopes ^{99m}Tc or ^{111}In would be more advantageous. Schmid et al. focused on the preparation of radiometal labeled thymidine complexes functionalized at position N3 with a DO3A-chelator suitable for radiolabeling with ^{111}In or lanthanide radioisotopes [243]. However, cellular uptake of the thymidine metal complexes in DoHH2 and HL60 cells failed. Clearly, there is an interest to develop thymidine derivatives suitable for radiolabeling with ^{99m}Tc. Celen et al. reported the preparation and evaluation of a ^{99m}Tc(V)-MAMA-propyl-thymidine complex as a potential probe for in vivo visualization of tumor cell proliferation via SPECT [46]. However, this ligand could not be phosphorylated because it was too bulky. The group of Schibli focused on the development of thymidine analogs labeled with the organometallic ^{99m}Tc-tricarbonyl-core (Fig. 7.16) [69, 276, 277]. The design of organometallic ^{99m}Tc-derivatives could be favorable as these complexes were sterically less demanding than previously prepared thymidine radiometal complexes. Those organometallic thymidine derivatives were systematically evaluated regarding the influence of the spacer length between the thymidine and the chelating system, the overall charge of the complex after radiometal coordination and the uptake in human neuroblastoma SKNMC cells. From these studies, it was concluded that neutral and anionic complexes are more readily accepted as substrates than cationic complexes.

Moreover, modeling experiments suggested that the flexibility of a longer spacer between the thymidine molecule and the organometallic core further improves the ability of the complex to be accommodated in the binding site of the enzyme. Cellular uptake was higher for complexes with log P values greater than one but still about 6-fold lower than for the ^{3}H-thymidine control compound. Although some of the organometallic thymidine complexes were identified as enzyme substrates, the low and often almost absent permeability of the thymidine metal complexes through the cellular membrane remains a major hurdle for these compounds.

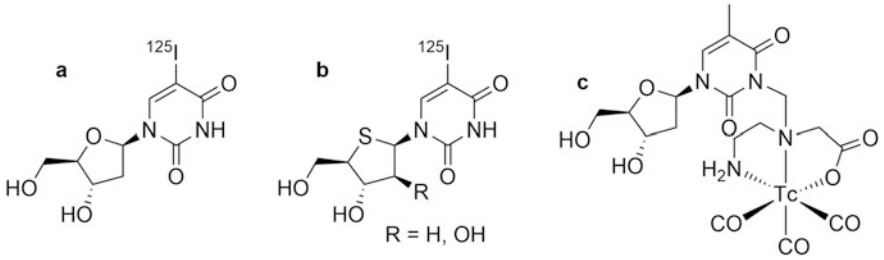

Fig. 7.16 Chemical structures of nucleoside-based SPECT tracers. **a** 5-[^{125}I]Iodo-2′-deoxyuridine ([^{125}I]IdUrd) [72, 255], **b** 5-[^{125}I]iodo-4′-thio-2′-deoxyuridine ([^{125}I]ITdU, R = H) and 5-[^{125}I]iodo-1-(4′-thio-*β*-arabinofuranosyl)-uracil ([^{125}I]ITAU, R = OH) [283] and **c** ^{99m}Tc(CO)$_3$-thymidine derivatives (n = 2, 3, 5 or 10) [69]

Iodinated thymidine analogs (e.g., 5-iodo-2′-deoxyuridine (IdUrd)) were used in another strategy as cell proliferation markers for nuclear imaging purposes and potential therapeutic application. However, the imaging quality was found to be impaired by the tracer's rapid in vivo degradation. Pre-application of 5-fluoro-2′-deoxyuridine (FdUrd) was tested with the aim to block thymidine synthesis and thus trigger the tumor uptake of [^{125}I]IdUrd [72]. Indeed, as a result of FdUrd pre-dosing [^{125}I]IdUrd incorporation into glioblastoma cells and tumors was increased and thus, the tumor-to-background contrast slightly improved. The same research group reported a beneficial effect of combining the administration of [^{125}I]IdUrd with unlabeled IdUrd to increase the rate of DNA incorporation of [^{125}I]IdUrd in malignant gliomas [73]. Apparently, the C–N-glycosidic bond of IdUrd is too labile in vivo which leads to metabolites that display reduced tumor affinity. In an attempt to increase the radiotracer's in vivo stability the tracer has been chemically modified by fluorination of the sugar moiety at different positions (3′ or 2′-substitution). However, the preparation of fluorine-stabilized iodinated thymidine analogs with retained cellular uptake, cytosolic phosphorylation, and selectivity for hTK1, appears to be quite challenging [97, 182]. A strategy for stabilizing the C–N-glycosidic bond without interfering with the cytosolic thymidine kinase has been carried out by the replacement of the furanose ring oxygen with sulfur for preparation of 5-[^{125}I]iodo-4′-thio-2′-deoxyuridine ([^{125}I]ITdU) and 5-[^{125}I]iodo-1-(4′-thio-β-D-arabinofuranosyl)uracil ([^{125}I]ITAU) (Fig. 7.16) [283]. ITdU exhibited high resistance to the glycosidic bond cleavage reaction provoked by thymidine phosphorylase, while maintaining affinity to nucleoside kinases. Also, the increased in vivo radioiodination stability and rapid DNA incorporation of ITdU resulted in a preferential uptake of radioactivity in the proliferating organs making this tracer a promising tumor-imaging agent. A comparative study of six 5-iodonucleosides revealed that the in vivo proliferation-imaging potential of nucleosides might be estimated by their in vitro affinity for TK1 and their C–N-glycosidic bond stability [284]. However, since these iodonucleosides have not been examined with regard to the important step of the nucleoside transport activity, further investigations would be necessary to allow a clear statement which radiotracer would be the most suitable for imaging of tumor cell proliferation.

By the examples of nucleoside derivatives and conjugates of carbohydrates, it was demonstrated that the development of radiotracers for intracellular targets might be problematic if bulky metal chelates are employed since cellular uptake of these radiotracers via transmembrane-spanning carriers or passive diffusion could be hindered.

7.6.3 Radioiodinated meta-Iodobenzylguanidine (MIBG)

Finally, we would like to highlight a long-serving but still frequently used tumor-imaging agent with an intracellular target. Meta-Iodobenzylguanidine (MIBG), a catecholamine analog, is suitable for radiolabeling with radioactive iodine (e.g., ^{123}I) for the purpose of SPECT imaging of neuroendocrine and carcinoid tumors, a subtype of neuroendocrine tumors [133]. Radiolabeled MIBG was first synthesized at the University of Michigan as early as 1980 [306]. It localizes through the physiologic nor-epinephrine reuptake mechanisms with uptake into catecholamine storage vesicles of adrenergic nerve ending and the cells of the adrenal medulla. Carcinoid tumor cells share the common characteristic of a sodium-dependent ATP/Mg^{2+} neuronal pump mechanism in their cell membranes that allows the accumulation of nor-epinephrine and MIBG where MIBG is not significantly metabolized. Initially, ^{131}I-labeled MIBG was used for the detection of neuroendocrine tumors such as pheochromocytomas, but later its application has been extended also to scintigraphic visualization of neuroblastoma and carcinoid tumors [44, 45, 52, 105, 258, 297].

Although both [^{123}I]MIBG and [^{131}I]MIBG can be used for the purpose of radionuclide imaging, ^{123}I has dosimetry and imaging characteristics superior to ^{131}I and thus, it is the preferred radionuclide for SPECT imaging (Fig. 7.17). In contrast, ^{131}I is preferred for therapy due to the emission of β-particles and dosimetric considerations [120].

To develop an MIBG analog with improved uptake in tumors, no-carrier-added [^{131}I]MIBG has been developed. The methodology for producing high specific activity (no-carrier-added) [^{131}I]MIBG was originally described in 1993, but only recently it has been developed for clinical application. With this method, nearly every molecule of MIBG contains an ^{131}I-radiolabel, whereas prior methods provided a mixture of the ^{131}I-tracer and the non-radioactive compound (with ^{127}I), wherein only 1 of 2,000 molecules of MIBG contained radioactive iodine. As a result of the high specific activity achieved by the no-carrier-added radiolabeling method, the mass of the MIBG administered can be reduced and thus undesired side-effects caused by the non-radioactive MIBG, such as hypertension during infusion could be minimized. The only concern of the no-carrier-added [^{131}I]MIBG has been that normal tissues and organs with relatively low levels of nor-epinephrine uptake might absorb more radioactivity because of the lack of competitive inhibition of radiotracer uptake by the non-radioactive MIBG.

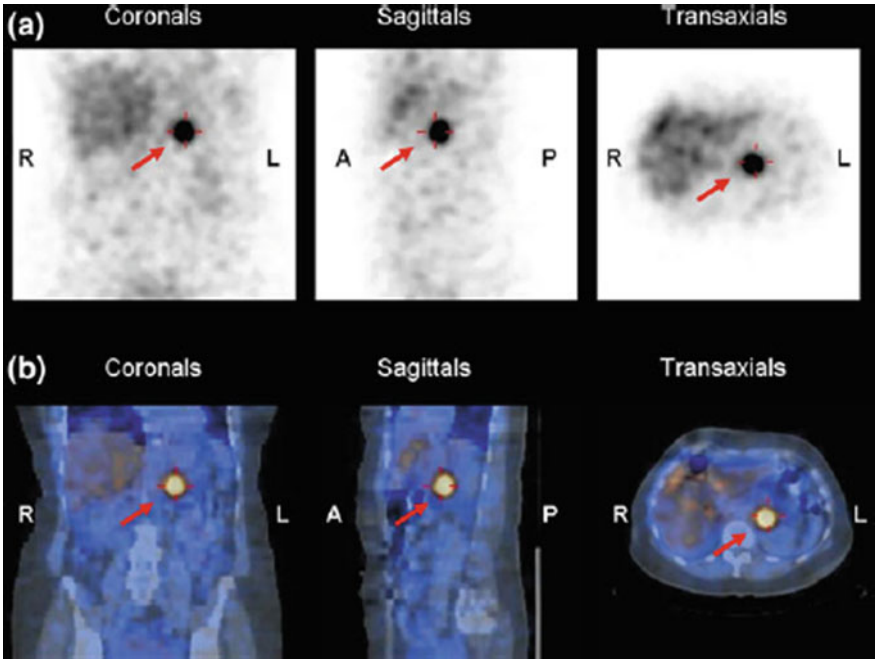

Fig. 7.17 SPECT images **a** and SPECT/CT overlay **b** of a patient with a neuroendocrine tumor (pheochromocytoma) in the upper thorax. Accumulation of [^{123}I]MIBG in the malignant tissue is indicated with *red arrows*. The images have been kindly provided by N. Schäfer, (MD, Ph.D.), University Hospital, Zurich, Switzerland

7.7 Glutamate-Ureido-Based Inhibitors of Prostate-Specific Membrane Antigen (PSMA)

Prostate-specific membrane antigen (PSMA) is a metallopeptidase expressed in epithelial cells of the prostate and highly overexpressed in 95% of advanced prostate cancers. PSMA is also known as glutamate carboypeptidase II (GCPII), folate hydrolase 1 (FOLH1), and *N*-acetyl-L-aspartyl-L-glutamate peptidase I (NAALADase). PSMA undergoes constitutive internalization, has no known ligand, is not specific to the prostate gland, and is expressed in other normal (e.g., salivary glands, duodenal mucosa, proximal renal tubular cells, and neuroendocrine cells in the colonic crypts) and neoplastic (e.g., transitional cell carcinoma, renal cell carcinoma, colon carcinoma, and endothelial cells of neovasculature) tissues [262].

PSMA can be selectively targeted using radiolabeled ligands based on urea-linked dipeptides, e.g., Glu-urea-Lys. These small-molecules binding the PSMA can be radiolabeled with γ-emitters like ^{99m}Tc and $^{123/131}$I or positron emitters like ^{68}Ga [3, 5, 22] and ^{18}F for diagnosis [99] as well as with their theranostic counterparts such as ^{177}Lu (γ-and β-emitter) or ^{225}Ac (α-emitter) for therapy [4, 122, 141, 221, 245]. Reviews summarizing the theranostic role of PSMA ligands for molecular imaging and targeted molecular radiotherapy have been published recently [2, 17, 137, 142, 220]. Here, the discussion is focused on the appropriate glutamate-ureido-based tracers labeled with ^{123}I or ^{99m}Tc.

7.7.1 ^{123}I- and ^{131}I-Labeled PSMA Radioligands

The use of low-molecular-weight PSMA ligands both for diagnosis and therapy began with the development of the ^{123}I- and ^{131}I-labeled PSMA inhibitors MIP-1072 and MIP-1095 [115, 116, 174]. Both tracers have very similar structures (Fig. 7.18) and comparable pharmacokinetics [50].

MIP-1095 can be used for SPECT imaging ([^{123}I]I-MIP-1095), PET imaging ([^{124}I]I-MIP-1095), and endoradionuclide therapy PSMA([^{131}I]I-MIP-1095-RLT). The first evaluation of [^{123}I]I-MIP-1095 for SPECT imaging in patients was described by Barrett et al. in 2013 [23]. Zechmann et al. reported dosimetry and therapy results using matched pair [^{124}I]I-MIP-1095 PET imaging and [^{131}I]I-MIP-1095 PSMA-RLT [316]. Afshar-Oromieh et al. evaluated toxicity and antitumor activity after single and repeated PSMA-targeting radioligand therapy of metastatic prostate cancer with [^{131}I]I-MIP-1095 [3, 5].

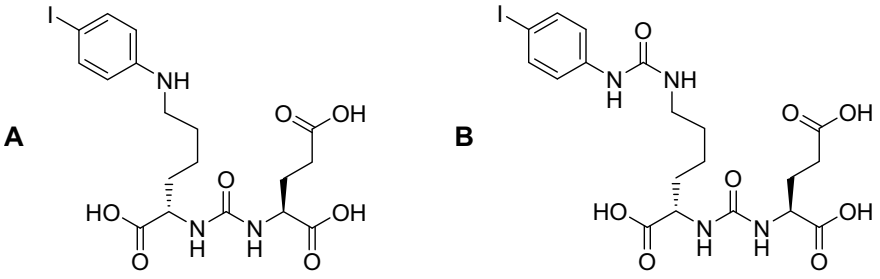

Fig. 7.18 Chemical structures of MIP-1072 (**a**) and MIP-1095 (**b**)

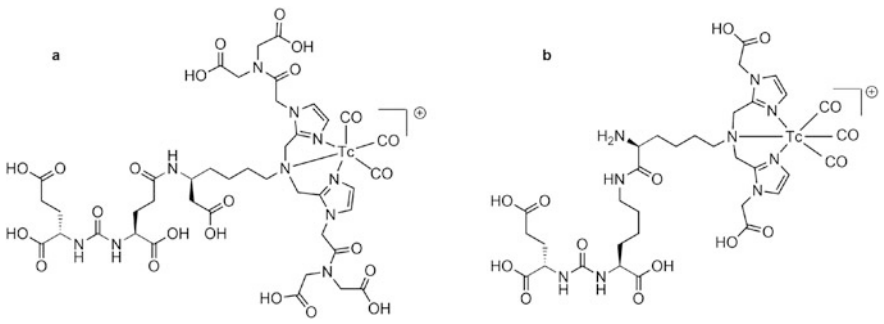

Fig. 7.19 Chemical structures of [^{99m}Tc]Tc-MIP-1404 (**a**) and [^{99m}Tc]Tc-MIP-1405 (**b**)

7.7.2 ^{99m}Tc-Labeled PSMA Radioligands

Several studies have been published dealing with the preclinical development of ^{99m}Tc-labeled PSMA radiotracers [166, 287]. The most promising agents among all ^{99m}Tc-labeled PSMA radiotracers are [^{99m}Tc]Tc-MIP-1404, also known as Trofolastat, and [^{99m}Tc]Tc-MIP-1405 (Fig. 7.19). Both compounds have been developed by Molecular Insight Pharmaceuticals (MIP) [117, 175]. The MIP structures contain single-amino-acid chelators (SAACs). Functionalized polar imidazole rings have been introduced in order to reduce lipophilicity and hepatobiliary excretion. ^{99m}Tc labeling follows the technetium tricarbonyl approach.

In preclinical studies [^{99m}Tc]Tc-MIP-1404 showed a fast clearance from the kidneys and non-target tissues while retained to the LNCaP tumor over 4 h. Furthermore, [^{99m}Tc]Tc-MIP-1404 also displayed the highest tumor-to-blood and tumor–to–skeletal muscle ratios [101, 117, 175]. [^{99m}Tc]Tc-MIP-1404 (Trofolastat) is the first PSMA imaging low-molecular-weight molecule that has been used in a phase-III clinical trials for noninvasive imaging of prostate cancer (European Union Trials Register EudraCT 2012-001864-30; ClinicalTrials.gov NCT02615067 [proSPECT-AS]).

A clinical database search from April 2013 to May 2017 yielding 93 patients with histologically confirmed cancer in whom SPECT/CT with [^{99m}Tc]Tc-MIP-1404 had been performed for primary whole-body staging before therapy [244, 245]. The authors claimed that imaging with this tracer has a high accuracy and low interobserver variability in the diagnosis of PC and allows detection of lymph node and bone metastases in a significant proportion of as yet untreated PC patients.

Recently two additional radiotracers have been introduced, [^{99m}Tc]Tc-PSMA-I&S [228, 303] and [^{99m}Tc]Tc-EDDA/HYNIC-iPSMA, where iPSMA stands for Lys(Nal)-Urea-Glu [84, 238]. The chemical structures are shown in Fig. 7.20. In a comparative analysis Lawal et al. evaluated the diagnostic sensitivity of SPECT/CT versus PET/CT in prostate carcinoma imaging using [^{99m}Tc]Tc-EDDA/HYNIC-iPSMA in comparison with [^{68}Ga]Ga-PSMA-11 [147].

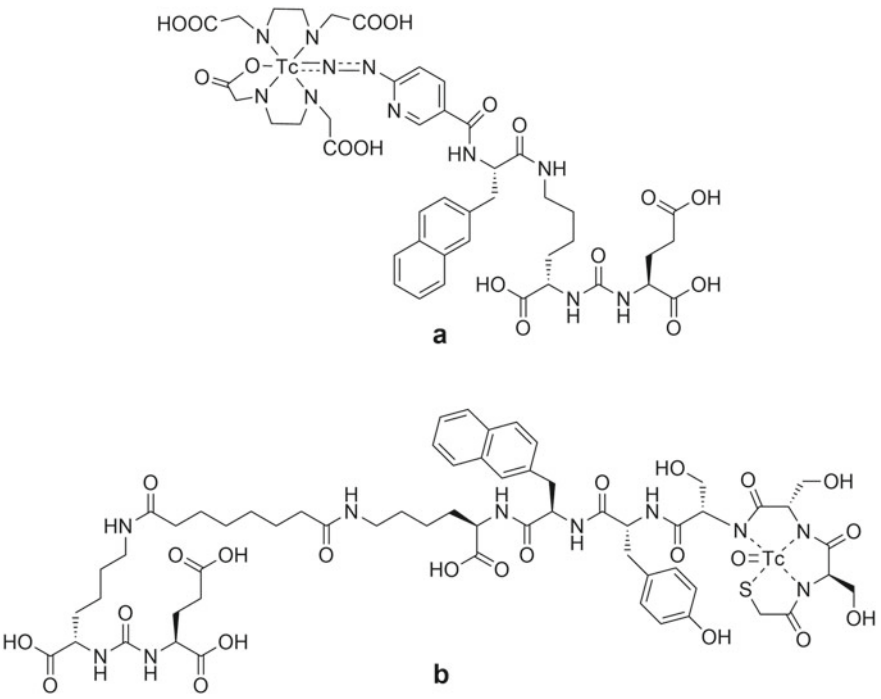

Fig. 7.20 Chemical structures of [^{99m}Tc]Tc-EDDA/HYNIC-iPSMA (**a**) and [^{99m}Tc]Tc-PSMA-I&S (**b**)

7.8 Sentinel Lymph Node (SNL) Localization

Detection of the sentinel lymph node (SNL), the first node to receive lymphatic flow as well as metastatic cells from the primary tumor site, is currently employed for planning the therapeutic treatment of cancers such as breast cancer and skin melanoma. Commonly, ^{99m}Tc-labeled colloids in combination with blue dyes are used to detect the sentinel lymph node. The labeled colloids are injected beneath the skin surrounding the primary tumor or alternatively directly into the tumor. After entering the lymphatic vessels, colloids use the same drainage pathway as potential metastatic cancer cells and are eventually retained in the first draining lymph node (sentinel node) by phagocytosis or mechanical trapping. However, colloidal radiopharmaceuticals such as ^{99m}Tc-sulfur colloid, ^{99m}Tc-antimony trisulfide, and ^{99m}Tc-labeled albumin microcolloids have disadvantages, like slow elimination rates from the injection site and migration to secondary nodes [208]. Thus, non-colloidal particles have been developed as alternatives such as ^{99m}Tc-labeled human serum albumin and ^{99m}Tc-labeled dextran.

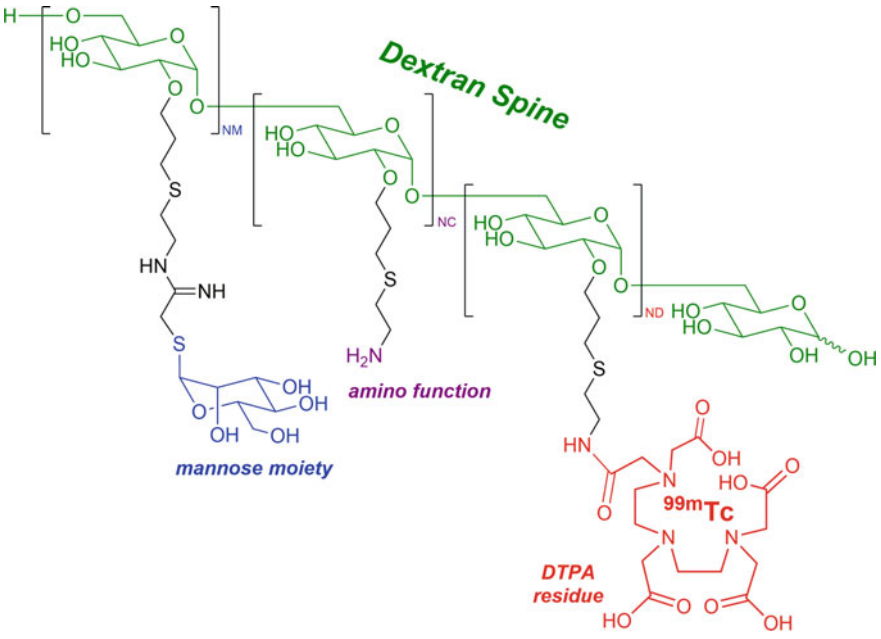

Fig. 7.21 Schematic representation of ^{99m}Tc-Tilmanocept for lymphatic mapping and Sentinel Lymph Node (SNL) localization. The unlabeled DTPA-mannosyl-dextran has a molecular weight of 35,800 g/mol and a molecular diameter of 7.1 nm. The final amino (NC), mannose (NM), and DTPA (ND) densities were 23, 55, and 8 mol per dextran [292]

A fluorescence-labeled ^{99m}Tc-HSA derivative (indocyanine green ICG-^{99m}Tc--NanoColl) was used to improve the surgical accuracy of laparoscopic lymph node (LN) dissection by integration of molecular imaging and intraoperative image guidance [290]. The authors could demonstrate that multimodal ICG-^{99m}Tc-NanoColloid, in combination with a laparoscopic fluorescence laparoscope, can be used to facilitate and optimize dissection of SLNs during robot-assisted laparoscopic prostatectomy.

^{99m}Tc-Tilmanocept (Lymphoseek), a tailor-made ^{99m}Tc-radiopharmaceutical for SLN diagnosis based on dextran has been approved by the FDA in 2013 [19, 21, 263, 278, 286, 292, 295]. It is a macromolecule (18 kDa, 7 nm size) composed of a dextran backbone and multiple subunits of DTPA and mannose (Fig. 7.21). ^{99m}Tc-Tilmanocept belongs to the class of receptor-binding radiopharmaceuticals. The mannose residues serve as ligands for receptors expressed on myeloid cells for recognition and binding. ^{99m}Tc-labeling of the macromolecule is performed via diethylenetriamine pentaacetic acid (DTPA). The structure of the Tc chelate is not exactly known.

Extending the diagnostic use of Tilmanocept an ^{111}In-labeled derivative was described to target mannose receptor expression on macrophages in atherosclerotic plaques of apolipoprotein E-knockout mice [291].

7.9 Optimization of SPECT Tracer Design and Potential Reasons for Failure

The design and development of a nuclear imaging probe independent of PET or SPECT comprises an appropriate biomolecule as targeting vector, a site for conjugation that does not interfere with the biomolecule's binding affinity to the tumor-associated target, a suitable linker length, and a radioisotope that matches with an appropriate biomolecule. For stable coordination of metallic radioisotopes, the choice of a suitable chelator is crucial. There are several possible strategies to optimize SPECT tracers with regard to their specificity to and selectivity for the targeted malignant tissue while minimizing their uptake in healthy tissues and organs. Variation of the radionuclide, modification of the bifunctional chelator, introduction of linker entities of variable spacer length for stabilization or modulation of the overall tracer characteristics, alteration of the radiolabeling technique and manipulation of the radiotracer's blood, and normal tissue clearance by variation of the biomolecule's overall size (e.g., antibodies versus antibody fragments or peptides). Finally, optimization of the tissue distribution of radiotracers might also be accomplished by a combination with non-radioactive substances whereof the most prominent example is the application of positively charged amino acids (e.g., lysine) that blocks renal uptake of radiolabeled Fab fragments of antibodies [28, 30] and peptides [61, 229, 294].

During the course of about two decades of (pre)clinical research with tumor-targeted SPECT tracers several reasons for potential failures of SPECT imaging agents could be identified (Table 7.4). Based on the data obtained with nuclear imaging agents that initially failed, new strategies to optimize the design and utility of SPECT tracers are currently being developed.

7.10 Summary and Conclusion

A variety of approaches for the design and improvement of SPECT tracers have been discussed herein. Each class of targeting agents, antibodies, peptides, and non-peptide-based small-molecules such as vitamins has its pros and cons for application in diagnostic nuclear medicine. In principle, it would be ideal to use SPECT tracers that accumulate specifically in malignancies and that are rapidly cleared via kidneys allowing high tumor-to-background contrast of radioactivity already short after administration. Such optimal characteristics are, however, not always easy to achieve.

The recent observation that somatostatin and bombesin analog antagonists provide superior characteristics over agonists with regard to their tumor accumulation is an unexpected finding that is not yet completely understood. Using oligomeric ligands to improve binding and targeting properties of radiolabeled peptides over their monomeric counterparts appears to be a more rational design that could be successfully proven, for example, with RGD-based analogs. Recently,

Table 7.4 Potential reasons for failure of tumor-targeted nuclear imaging

Possibilities for failure	Consequences	Examples
Expression of the target structure in normal tissues and organs	Radiotracer accumulation in normal tissues and organs	– Bombesin receptor (pancreas) – Somatostatin receptor (adrenals) – Folate receptor (kidneys)
Long circulation time	High background radiation in the blood—dose burden to healthy tissues (bone marrow)	– Monoclonal antibodies
Short circulation time	Low tumor accumulation	– Small-molecular-weight targeting agents (e.g., folic acid)
Rapid enzymatic metabolism	Low tumor accumulation of metabolites in kidneys and liver	– Non-stabilized neurotensin analogs
Binding to physiological transport proteins	High background radiation in the blood	– Vitamin B_{12}/transcobalamin II
Intracellular targets	Cellular uptake via carrier systems or passive diffusion hindered by bulky radiometal complexes	– ^{99m}Tc-glucose analogs – ^{99m}Tc-thymidine analogs
Lipophilic character	Unspecific accumulation of the radiotracer in the bile, liver, and intestinal tract	– $^{99m}Tc(CO)_3$-moiety – Alkyl chain-spacers
Low-specific activity	Low tumor uptake undesired side-effects as a result of substantial amount of injected "cold" tracer	– [^{131}I]MIBG

vitamin-based radio imaging agents have been developed that are selectively accumulated in tumor cells. In the case of vitamin B_{12}, analogs with abolished binding to the ubiquitous protein transcobalalmin II showed a reduced uptake in non-targeted tissues. In the case of FR-targeting, it was the combined application with the antifolate pemetrexed that led to an improved tumor selectively of folic acid-based radioconjugates while undesired uptake in FR-positive kidneys could be reduced. Targeting of intracellular tumor markers such as the enzymes hexokinase or human thymidine kinase 1 turned out to be a more problematic strategy for SPECT tracers, particularly those that are based on radiometals, compared to the targeting of cell surface-exposed tumor markers. The necessity of the targeting agent to permeate cancer cell membranes via carrier systems or passive diffusion to reach intracellular targets could be a hindrance for a proper function of the targeting system in particular if the radioconjugate is composed of a bulky radiometal complex.

Finally, it has to be critically acknowledged that only a small selection of examples for tracer designs could be included in this chapter. The immense opportunities for the design of radiopharmaceuticals and the enormous potential it

provides for future development of new and improved SPECT tracers holds great promise for early clinical application of novel imaging agents in oncology.

References

1. Abrams MJ, Juweid M et al (1990) Technetium-99m-human polyclonal IgG radiolabeled via the hydrazino nicotinamide derivative for imaging focal sites of infection in rats. J Nucl Med 31:2022–2028
2. Afshar-Oromieh A, Babich JW et al (2016) The rise of PSMA ligands for diagnosis and therapy of prostate cancer. J Nucl Med 57(S3):79S–89S
3. Afshar-Oromieh A, Haberkorn U et al (2017) Repeated PSMA-targeting radioligand therapy of metastatic prostate cancer with ^{131}I-MIP-1095. Eur J Nucl Med Mol Imaging 44:950–959
4. Afshar-Oromieh A, Hetzheim H et al (2015) The theranostic PSMA Ligand PSMA-617 in the diagnosis of prostate cancer by PET/CT: biodistribution in humans, radiation dosimetry, and first evaluation of tumor lesions. J Nucl Med 56:1697–1705
5. Afshar-Oromieh A, Holland-Letz T et al (2017) Diagnostic performance of ^{68}Ga-PSMA-11 (HBED-CC) PET/CT in patients with recurrent prostate cancer: evaluation in 1007 patients. Eur J Nucl Med Mol Imaging 44:1258–1268
6. Alberto R, Ortner K et al (2001) Synthesis and properties of boranocarbonate: a convenient in situ CO source for the aqueous preparation of $[^{99m}Tc(OH_2)_3(CO)_3]^+$. J Am Chem Soc 123:3135–3136
7. Alberto R, Schibli R et al (1998) A novel organometallic aqua complex of technetium for the labeling of biomolecules: synthesis of $[^{99m}Tc(OH_2)_3(CO)_3]^+$ from $[^{99m}TcO_4]^-$ in aqueous solution and its reaction with a bifunctional ligand. J Am Chem Soc 120:7987–7988
8. Alberto R, Schibli R et al (1999) First application of *fac*-$[^{99m}Tc(OH_2)_3(CO)_3]^+$ in bioorganometallic chemistry: design, structure, and in vitro affinity of a 5-HT1A receptor ligand labeled with ^{99m}Tc. J Am Chem Soc 121:6076–6077
9. Alberto R, Schibli R et al (1999) Basic aqueous chemistry of $[M(OH_2)_3(CO)_3]^+$ (M = Re, Tc) directed towards radiopharmaceutical application. Coord Chem Rev 192:901–919
10. Alford R, Ogawa M et al (2009) Molecular probes for the in vivo imaging of cancer. Mol BioSyst 5:1279–1291
11. Alshoukr F, Rosant C et al (2009) Novel neurotensin analogues for radioisotope targeting to neurotensin receptor-positive tumors. Bioconjug Chem 20:1602–1610
12. Alves S, Correia JD et al (2006) Pyrazolyl conjugates of bombesin: a new tridentate ligand framework for the stabilization of *fac*-$[M(CO)_3]^+$ moiety. Nucl Med Biol 33:625–634
13. Antony AC (1996) Folate receptors. Ann Rev Nutr 16:501–521
14. Aranda-Lara L, Ferro-Flores G et al (2016) Synthesis and evaluation of Lys1(α, γ-Folate) Lys3(177Lu-DOTA)-Bombesin(1–14) as a potential theranostic radiopharmaceutical for breast cancer. Appl Radiat Isot 107:214–219
15. Artiko V, Afgan A et al (2016) Evaluation of neuroendocrine tumors with ^{99m}Tc-EDDA/-HYNIC TOC. Nucl Med Rev 19:99–103
16. Assaraf YG, Leamon CP et al (2014) The folate receptor as a rational therapeutic target for personalized cancer treatment. Drug Resist Updates 17:89–95
17. Awang ZH, Essler M et al (2018) Radioligand therapy of metastatic castration-resistant prostate cancer: current approaches. Radiat Oncol 13:98
18. Axworthy DB, Reno JM et al (2000) Cure of human carcinoma xenografts by a single dose of pretargeted yttrium-90 with negligible toxicity. Proc Natl Acad Sci USA 97:1802–1807
19. Azad AK, Rajaram MVS et al (2015) Tilmanocept, a new radiopharmaceutical tracer for cancer sentinel lymph nodes, binds to the mannose receptor (CD206). J Immunol 195:2019–2029

20. Baidoo KE, Lin KS et al (1998) Design, synthesis, and initial evaluation of high-affinity technetium bombesin analogues. Bioconjug Chem 9:218–225
21. Baker JL, Pu M et al (2015) Comparison of [^{99m}Tc]Tilmanocept and filtered [^{99m}Tc]Sulfur colloid for identification of SLNs in breast cancer patients. Ann Surg Oncol 22:40–45
22. Baranski AC, Schäfer M et al (2017) Improving the imaging contrast of ^{68}Ga-PSMA-11 by targeted linker design: charged spacer moieties enhance the pharmacokinetic properties. Bioconjugate Chem 28:2485–2492
23. Barrett JA, Coleman RE et al (2013) First-in-man evaluation of 2 high-affinity PSMA-avid small molecules for imaging prostate cancer. J Nucl Med 54:380–387
24. Bartholoma MD, Louie AS et al (2010) Technetium and gallium derived radiopharmaceuticals: comparing and contrasting the chemistry of two important radiometals for the molecular imaging era. Chem Rev 110:2903–2920
25. Bauer JA, Morrison BH et al (2002) Effects of interferon beta on transcobalamin II-receptor expression and antitumor activity of nitrosylcobalamin. J Natl Cancer Inst 94:1010–1019
26. Bayly SR, Fisher CL et al (2004) Carbohydrate conjugates for molecular imaging and radiotherapy: ^{99m}Tc(I) and ^{186}Re(I) tricarbonyl complexes of N-(2′-hydroxybenzyl)-2-amino-2-deoxy-D-glucose. B. Bioconjug Chem 15:923–926
27. Begent RH, Verhaar MJ et al (1996) Clinical evidence of efficient tumor targeting based on single-chain Fv antibody selected from a combinatorial library. Nat Med 2:979–984
28. Behr TM, Becker WS et al (1996) Reduction of renal uptake of monoclonal antibody fragments by amino acid infusion. J Nucl Med 37:829–833
29. Behr TM, Gotthardt M et al (2001) Imaging tumors with peptide-based radioligands. Q J Nucl Med 45:189–200
30. Behr TM, Sharkey RM et al (1995) Reduction of the renal uptake of radiolabeled monoclonal antibody fragments by cationic amino acids and their derivatives. Cancer Res 55:3825–3834
31. Bernard BF, Krenning EP et al (1997) D-lysine reduction of indium-111 octreotide and yttrium-90 octreotide renal uptake. J Nucl Med 38:1929–1933
32. Birchler MT, Thuerl C et al (2007) Immunoscintigraphy of patients with head and neck carcinomas, with an anti-angiogenetic antibody fragment. Otolaryngol Head Neck Surg 136:543–548
33. Blomquist L, Flodh H et al (1969) Uptake of labelled vitamin B12 and 4-iodophenylalanine in some tumors of mice. Experientia 25:294–296
34. Boeggeman E, Ramakrishnan B et al (2009) Site specific conjugation of fluoroprobes to the remodeled Fc N-glycans of monoclonal antibodies using mutant glycosyltransferases: application for cell surface antigen detection. Bioconjug Chem 20:1228–1236
35. Boerman OC, van Schaijk FG et al (2003) Pretargeted radioimmunotherapy of cancer: progress step by step. J Nucl Med 44:400–411
36. Brack SS, Dinkelborg LM et al (2004) Molecular targeting of angiogenesis for imaging and therapy. Eur J Nucl Med Mol Imaging 31:1327–1341
37. Breeman WA, de Jong M et al (2002) Preclinical comparison of ^{111}In-labeled DTPA- or DOTA-bombesin analogs for receptor-targeted scintigraphy and radionuclide therapy. J Nucl Med 43:1650–1656
38. Brekken RA, Huang X et al (1998) Vascular endothelial growth factor as a marker of tumor endothelium. Cancer Res 58:1952–1959
39. Bruehlmeier M, Garayoa EG et al (2002) Stabilization of neurotensin analogues: effect on peptide catabolism, biodistribution and tumor binding. Nucl Med Biol 29:321–327
40. Buchmann I, Vogg AT et al (2003) [^{18}F]5-fluoro-2-deoxyuridine-PET for imaging of malignant tumors and for measuring tissue proliferation. Cancer Biother Radiopharm 18:327–337
41. Buchsbaum DJ (1995) Experimental approaches to increase radiolabeled antibody localization in tumors. Cancer Res 55:5729s–5732s

42. Buchsbaum DJ (1997) Experimental tumor targeting with radiolabeled ligands. Cancer 80:2371–2377
43. Carnemolla B, Neri D et al (1996) Phage antibodies with pan-species recognition of the oncofoetal angiogenesis marker fibronectin ED-B domain. Int J Cancer 68:397–405
44. Carrasquillo JA, Pandit-Taskar N et al (2016) I-131-metaiodobenzylguanidine therapy of pheochromocytoma and paraganglioma. Semin Nucl Med 46:203–214
45. Carrasquillo JA, Pandit-Taskar et al (2012) Radionuclide therapy of adrenal tumors. J Surg Oncol 06:632–642
46. Celen S, de Groot T et al (2007) Synthesis and evaluation of a ^{99m}Tc-MAMA-propyl-thymidine complex as a potential probe for in vivo visualization of tumor cell proliferation with SPECT. Nucl Med Biol 34:283–291
47. Cescato R, Erchegyi J et al (2008) Design and in vitro characterization of highly sst2-selective somatostatin antagonists suitable for radiotargeting. J Med Chem 51:4030–4037
48. Cescato R, Schulz S et al (2006) Internalization of sst2, sst3, and sst5 receptors: effects of somatostatin agonists and antagonists. J Nucl Med 47:502–511
49. Chen Q, Ma Q et al (2015) An exploratory study on ^{99m}Tc-RGDBBN peptide scintimammography in the assessment of breast malignant lesions compared to ^{99m}Tc-3P4-RGD2. PLoS ONE 10:e0123401
50. Chopra A (2009) ^{123}I-Labeled (S)-2-(3-((S)-1-carboxy-5-(4-iodobenzylamino)-pentyl) ureido)-pentanedoic acid. In: Molecular imaging and contrast agent database (MICAD) [Internet]. bethesda (MD): national center for biotechnology information (US); 2004–2013
51. Christ E, Wild D et al (2009) Glucagon-like peptide-1 receptor imaging for localization of insulinomas. J Clin Endocrinol Metab 94:4398–4405
52. Cistaro A, Quartuccio N et al (2015) ^{124}I-MIBG: a new promising positron-emitting radiopharmaceutical for the evaluation of neuroblastoma. Nucl Med Rev 18:102–106
53. Collins DA, Hogenkamp HP (1997) Transcobalamin II receptor imaging via radiolabeled diethylene-triaminepentaacetate cobalamin analogs. J Nucl Med 38:717–723
54. Collins DA, Hogenkamp HP et al (1999) Tumor imaging via indium-111-labeled DTPA-adenosylcobalamin. Mayo Clin Proc 74:687–691
55. Collins DA, Hogenkamp HP et al (2000) Biodistribution of radiolabeled adenosylcobalamin in patients diagnosed with various malignancies. Mayo Clin Proc 75:568–580
56. Dapueto R, Castelli R et al (2011) Biological evaluation of glucose and deoxyglucose derivatives radiolabeled with $[^{99m}Tc(CO)_3(H_2O)_3]^+$ core as potential melanoma imaging agents. Bioorg Med Chem Lett 21:7102–7106
57. Dapueto R, Aguiar RB et al (2015) Technetium glucose complexes as potential cancer imaging agents. Bioorg Med Chem Lett 25:4254–4259
58. de Barros ALB, Cardoso VN et al (2010) Synthesis and biodistribution studies of carbohydrate derivatives radiolabeled with technetium-99m. Bioorg Med Chem Lett 20:315–317
59. de Barros ALB, das Gracas Mota L et al (2012) Kit formulation for ^{99m}Tc-labeling of HYNIC-βAla-Bombesin(7–14). Appl Radiat Isot 70:2440–2445
60. de Jong M, Bakker WH et al (1999) Preclinical and initial clinical evaluation of ^{111}In-labeled nonsulfated CCK8 analog: a peptide for CCK-B receptor-targeted scintigraphy and radionuclide therapy. J Nucl Med 40:2081–2087
61. de Jong M, Rolleman EJ et al (1996) Inhibition of renal uptake of indium-111-DTPA-octreotide in vivo. J Nucl Med 37:1388–1392
62. de Visser M, Bernard HF et al (2007) Novel ^{111}In-labelled bombesin analogues for molecular imaging of prostate tumours. Eur J Nucl Med Mol Imaging 34:1228–1238
63. de Visser M, Janssen PJ et al (2003) Stabilised ^{111}In-labelled DTPA- and DOTA-conjugated neurotensin analogues for imaging and therapy of exocrine pancreatic cancer. Eur J Nucl Med Mol Imaging 30:1134–1139

64. Decristoforo C, Mather SJ (2002) The influence of chelator on the pharmacokinetics of ^{99m}Tc-labelled peptides. Q J Nucl Med 46:195–205
65. Decristoforo C, Mather SJ et al (2000) ^{99m}Tc-EDDA/HYNIC-TOC: a new ^{99m}Tc-labelled radiopharmaceutical for imaging somatostatin receptor-positive tumours; first clinical results and intra-patient comparison with ^{111}In-labelled octreotide derivatives. Eur J Nucl Med 27:1318–1325
66. Decristoforo C, Melendez-Alafort L et al (2000) ^{99m}Tc-HYNIC-[Tyr^3]-octreotide for imaging somatostatin-receptor-positive tumors: preclinical evaluation and comparison with ^{111}In-octreotide. J Nucl Med 41:1114–1119
67. Delgado R, da Silva JJ (1982) Metal complexes of cyclic tetra-azatetra-acetic acids. Talanta 29:815–822
68. Demartis S, Tarli L et al (2001) Selective targeting of tumour neovasculature by a radiohalogenated human antibody fragment specific for the ED-B domain of fibronectin. Eur J Nucl Med 28:534–539
69. Desbouis D, Struthers H et al (2008) Synthesis, in vitro, and in silico evaluation of organometallic technetium and rhenium thymidine complexes with retained substrate activity toward human thymidine kinase type 1. J Med Chem 51:6689–6698
70. Dong C, Yang S et al (2016) SPECT/NIRF dual modality imaging for detection of intraperitoneal colon tumor with an avidin/biotin pretargeting system. Sci Rep 6:18905
71. Dumas C, Schibli R et al (2003) Versatile routes to C-2- and C-6-functionalized glucose derivatives of iminodiacetic acid. J Org Chem 68:512–518
72. Dupertuis YM, Vazquez M et al (2001) Fluorodeoxyuridine improves imaging of human glioblastoma xenografts with radiolabeled iododeoxyuridine. Cancer Res 61:7971–7977
73. Dupertuis YM, Xiao WH et al (2002) Unlabelled iododeoxyuridine increases the rate of uptake of [^{125}I]iododeoxyuridine in human xenografted glioblastomas. Eur J Nucl Med Mol Imaging 29:499–505
74. Edwards DS, Liu S et al (1997) New and versatile ternary ligand system for technetium radiopharmaceuticals: water soluble phosphines and tricine as coligands in labeling a hydrazinonicotinamide-modified cyclic glycoprotein IIb/IIIa receptor antagonist with ^{99m}Tc. Bioconjug Chem 8:146–154
75. Egli A, Alberto R et al (1999) Organometallic ^{99m}Tc-aquation labels peptide to an unprecedented high specific activity. J Nucl Med 40:1913–1917
76. Egli A, Hegetschweiler K et al (1997) Hydrolysis of the organometallic aqua ion *fac*-triaquatricarbonylrhenium(I). Mechanism, pK_a, and formation constants of the polynuclear hydrolysis products. Organometallics 16:1833–1840
77. Fan G, Wan R et al (2018) The distribution and imaging of ^{99m}Tc-nGO-PEG-FA in human Patu8988 tumor-bearing nude mice. Cancer Biother Radiopharm 33:445–459
78. Farkas R, Siwowska et al (2016) ^{64}Cu- and ^{68}Ga-based PET imaging of folate receptor-positive tumors: development and evaluation of an albumin-binding. Mol Pharm 13:1979–1987
79. Fernández M, Javaid F, Chudasama (2018) Advances in targeting the folate receptor in the treatment/imaging of cancers. Chem Sci 9:790–810
80. Ferreira CL, Bayly SR et al (2006) Carbohydrate-appended 3-hydroxy-4-pyridinone complexes of the $[M(CO)_3]^+$ core (M = Re, ^{99m}Tc, ^{186}Re). Bioconjug Chem 17:1321–1329
81. Ferreira CL, Ewart CB et al (2006) Glucosamine conjugates of tricarbonylcyclopentadienyl rhenium(I) and technetium(I) cores. Inorg Chem 45:6979–6987
82. Ferreira CL, Marques FL et al (2010) Cationic technetium and rhenium complexes with pendant carbohydrates. Appl Radiat Isot 68:1087–1093
83. Ferro-Flores G, Arteaga de Murphy C et al (2006) Preparation and evaluation of ^{99m}Tc-EDDA/HYNIC-[Lys^3]-bombesin for imaging gastrin-releasing peptide receptor-positive tumours. Nucl Med Commun 27:371–376
84. Ferro-Flores G, Luna-Gutiérrez M et al (2017) Clinical translation of a PSMA inhibitor for ^{99m}Tc-based SPECT. Nucl Med Biol 48:36–44

85. Ferro-Flores G, Rivero IA et al (2010) Click chemistry for [^{99m}Tc(CO)$_3$] labeling of Lys^3-bombesin. Appl Radiat Isot 68:2274–2278
86. Fischer CA, Vomstein S, Mindt TL (2014) A bombesin-shepherdin radioconjugate designed for combined extra- and intracellular targeting. Pharmaceuticals 7:662–675
87. Fisher RE, Siegel BA et al (2008) Exploratory study of ^{99m}Tc-EC20 imaging for identifying patients with folate receptor-positive solid tumors. J Nucl Med 49:899–906
88. Flodh H (1968) Autoradiographic studies on distribution of radiocobalt chloride in pregnant mice. Acta Radiol Ther Phys Biol 7:121–128
89. Flodh H, Ullberg S (1968) Accumulation of labelled vitamin B_{12} in some transplanted tumours. Int J Cancer 3:694–699
90. Garai I, Barna S et al (2016) Limitations and pitfalls of ^{99m}Tc-EDDA/HYNIC-TOC (Tektrotyd) scintigraphy. Nucl Med Rev 19:93–98
91. Garcia Garayoa E, Ruegg D et al (2007) Chemical and biological characterization of new Re(CO)$_3$/[^{99m}Tc](CO)$_3$ bombesin analogues. Nucl Med Biol 34:17–28
92. Garcia Garayoa E, Schweinsberg C et al (2007) New [^{99m}Tc]bombesin analogues with improved biodistribution for targeting gastrin releasing-peptide receptor-positive tumors. Q J Nucl Med Mol Imaging 51:42–50
93. Garcia Garayoa E, Schweinsberg C et al (2008) Influence of the molecular charge on the biodistribution of bombesin analogues labeled with the [^{99m}Tc(CO)$_3$]-core. Bioconjug Chem 19:2409–2416
94. Garcia-Garayoa E, Blauenstein P et al (2009) A stable neurotensin-based radiopharmaceutical for targeted imaging and therapy of neurotensin receptor-positive tumours. Eur J Nucl Med Mol Imaging 36:37–47
95. Garcia-Garayoa E, Maes V et al (2006) Double-stabilized neurotensin analogues as potential radiopharmaceuticals for NTR-positive tumors. Nucl Med Biol 33:495–503
96. Gardelle O, Roelcke U et al (2001) [^{76}Br]Bromodeoxyuridine PET in tumor-bearing animals. Nucl Med Biol 28:51–57
97. Gati WP, Misra HK et al (1984) Structural modifications at the 2′- and 3′-positions of some pyrimidine nucleosides as determinants of their interaction with the mouse erythrocyte nucleoside transporter. Biochem Pharmacol 33:3325–3331
98. Giblin MF, Veerendra B et al (2005) Radiometallation of receptor-specific peptides for diagnosis and treatment of human cancer. Vivo 19:9–29
99. Giesel FL, Will L et al (2018) Biochemical recurrence of prostate cancer: initial results with [^{18}F]PSMA-1007 PET/CT. J Nucl Med 59(4):632–635
100. Ginj M, Zhang H et al (2006) Radiolabeled somatostatin receptor antagonists are preferable to agonists for in vivo peptide receptor targeting of tumors. Proc Natl Acad Sci USA 103:16436–16441
101. Goffin KE, Joniau S et al (2017) Phase 2 Study of ^{99m}Tc-Trofolastat SPECT/CT to identify and localize prostate cancer in intermediate- and high-risk patients undergoing radical prostatectomy and extended pelvic LN dissection. J Nucl Med 58:1408–1413
102. Goldenberg DM, Rossi EA et al (2008) Multifunctional antibodies by the dock-and-lock method for improved cancer imaging and therapy by pretargeting. J Nucl Med 49:158–163
103. Good S, Walter MA et al (2008) Macrocyclic chelator-coupled gastrin-based radiopharmaceuticals for targeting of gastrin receptor-expressing tumours. Eur J Nucl Med Mol Imaging 35:1868–1877
104. Gotthardt M, van Eerd-Vismale J et al (2007) Indication for different mechanisms of kidney uptake of radiolabeled peptides. J Nucl Med 48:596–601
105. Grünwald F, Ezziddin S (2010) ^{131}I-metaiodobenzylguanidine therapy of neuroblastoma and other neuroendocrine tumors. Semin Nucl Med 40:153–163
106. Gugger M, Reubi JC (1999) Gastrin-releasing peptide receptors in non-neoplastic and neoplastic human breast. Am J Pathol 155:2067–2076

107. Guo W, Hinkle GH et al (1999) ^{99m}Tc-HYNIC-folate: a novel receptor-based targeted radiopharmaceutical for tumor imaging. J Nucl Med 40:1563–1569
108. Guo Z, Zhang P et al (2014) Synthesis and preliminary evaluation of novel ^{99m}Tc-labeled folate derivative via click reaction for SPECT imaging. Appl Radiat Isot 91:24–30
109. Guo Z, You L et al (2017) Development of a new FR-targeting Agent ^{99m}Tc-HYNFA with improved imaging contrast and comparison of multimerization and/or PEGylation strategies for radio-folate modification. Mol Pharm 14:3780–3788
110. Hamblett KJ, Press OW et al (2005) Role of biotin-binding affinity in streptavidin-based pretargeted radioimmunotherapy of lymphoma. Bioconjug Chem 16:131–138
111. Hammond PJ, Wade AF et al (1993) Amino acid infusion blocks renal tubular uptake of an indium-labelled somatostatin analogue. Br J Cancer 67:1437–1439
112. Hankus J, Tomaszewska R (2016) Neuroendocrine neoplasms and somatostatin receptor subtypes expression. Nucl Med Rev 19:111–117
113. Hekman MCH, Boerman OC et al (2017) Improved intraoperative detection of ovarian cancer by folate receptor alpha targeted dual-modality imaging. Mol Pharm 14:3457–3463
114. Heppeler A, Froidevaux S et al (1999) Radiometal-labelled macrocyclic chelator-derivatised somatostatin analogue with superb tumour-targeting properties and potential for receptor-mediated internal radiotherapy. Chem-Eur J 5:1974–1981
115. Hillier SM, Kern AM et al (2011) ^{123}I-MIP-1072, a small-molecule inhibitor of prostate-specific membrane antigen, is effective at monitoring tumor response to taxane therapy. J Nucl Med 52:1087–1093
116. Hillier SM, Maresca KP et al (2009) Preclinical evaluation of novel glutamate-urea-lysine analogues that target prostate-specific membrane antigen as molecular imaging pharmaceuticals for prostate cancer. Can Res 69:6932–6940
117. Hillier SM, Maresca KP et al (2013) ^{99m}Tc-labeled small-molecule inhibitors of prostate-specific membrane antigen for molecular imaging of prostate cancer. J Nucl Med 54:1369–1376
118. Hnatowich DJ, Virzi F (1987) Investigations of avidin and biotin for imaging applications. J Nucl Med 28:1294–1302
119. Ho C-L, Liu I-H et al (2011) Molecular imaging, pharmacokinetics, and dosimetry of ^{111}In-AMBA in human prostate tumor-bearing mice. J Biomed Biotechnol 2011:Article ID 101497. https://doi.org/10.1155/2011/101497
120. Hoefnagel CA, den Hartog Jager FC et al (1987) The role of ^{131}I-MIBG in the diagnosis and therapy of carcinoids. Eur J Nucl Med 13:187–191
121. Hoffman TJ, Gali H et al (2003) Novel series of ^{111}In-labeled bombesin analogs as potential radiopharmaceuticals for specific targeting of gastrin-releasing peptide receptors expressed on human prostate cancer cells. J Nucl Med 44:823–831
122. Hofman MS, Violet J et al (2018) [^{177}Lu]-PSMA-617 radionuclide treatment in patients with metastatic castration-resistant prostate cancer (LuPSMA trial): a single-centre, single-arm, phase 2 study. Lancet Oncol 19:825–833
123. Hong H, Sun J et al (2008) Radionuclide-based cancer imaging targeting the carcinoembryonic antigen. Biomark Insights 3:435–451
124. Jeong JM, Kinuya S et al (1994) Application of high affinity binding concept to radiolabel avidin with Tc-99m labeled biotin and the effect of pI on biodistribution. Nucl Med Biol 21:935–940
125. Ji T, Sun Y et al (2015) The diagnostic role of ^{99m}Tc-dual receptor targeted probe and targeted peptide bombesin (RGD-BBN) SPET/CT in the detection of malignant and benign breast tumors and axillary lymph nodes compared to ultrasound. Hell J Nucl Med 18:108–113
126. Ji T, Gao S (2016) ^{99m}Tc-Glu-c(RGDyK)-bombesin SPECT can reduce unnecessary biopsy of masses that are BI-RADS category 4 on ultrasonography. J Nucl Med 57:1196–1200

127. Johnson CV, Shelton T et al (2006) Evaluation of combined ^{177}Lu-DOTA-8-AOC-BBN (7-14)NH^2 GRP receptor-targeted radiotherapy and chemotherapy in PC-3 human prostate tumor cell xenografted SCID mice. Cancer Biother Radiopharm 21:155–166
128. Josten A, Haalck L et al (2000) Use of microbial transglutaminase for the enzymatic biotinylation of antibodies. J Immunol Methods 240:47–54
129. Kastner ME, Lindsay MJ et al (1982) Synthesis and structure of trans-$[O_2(en)2Tc^v]^+$. Inorg Chem 21:2037–2040
130. Ke CY, Mathias CJ et al (2003) The folate receptor as a molecular target for tumor-selective radionuclide delivery. Nucl Med Biol 30:811–817
131. Ke CY, Mathias CJ et al (2004) Folate-receptor-targeted radionuclide imaging agents. Adv Drug Deliv Rev 56:1143–1160
132. Khan IU, Shahid A et al (2016) Development and bioevaluation of $^{99m}Tc(CO)_3$-labeled (1-azido-1-deoxy-β-D-glucopyranoside) complex as a potential tumor-seeking agent. Pak J Pharm Sci 29:213–219
133. Khan MU, Morse M et al (2008) Radioiodinated metaiodobenzylguanidine in the diagnosis and therapy of carcinoid tumors. Q J Nucl Med Mol Imaging 52:441–454
134. King DJ, Turner A et al (1994) Improved tumor targeting with chemically cross-linked recombinant antibody fragments. Cancer Res 54:6176–6185
135. Kobayashi H, Sakahara H et al (1994) Improved clearance of radiolabeled biotinylated monoclonal antibody following the infusion of avidin as a "chase" without decreased accumulation in the target tumor. J Nucl Med 35:1677–1684
136. Koch P, Mäcke HR (1992) ^{99m}Tc Labeled Biotin Conjugate in a Tumor "Pretargeting" Approach with Monoclonal Antibodies. Angew Chem Int Ed 31:1507–1509
137. Kopka K, Benešová M et al (2017) Glu-ureido-based inhibitors of prostate-specific membrane antigen: lessons learned during the development of a novel class of low-molecular-weight theranostic radiotracers. J Nucl Med 58(Suppl 2):17S–26S
138. Körner M, Stockli M et al (2007) GLP-1 receptor expression in human tumors and human normal tissues: potential for in vivo targeting. J Nucl Med 48:736–743
139. Knight JC, Cornelissen B (2014) Bioorthogonal chemistry: implications for pretargeted nuclear (PET/SPECT) imaging and therapy. Am J Nucl Med Mol Imaging 4:96–113
140. Knox SJ, Goris ML et al (2000) Phase II trial of yttrium-90-DOTA-biotin pretargeted by NR-LU-10 antibody/streptavidin in patients with metastatic colon cancer. Clin Cancer Res 6:406–414
141. Kratochwil C, Bruchertseifer F et al (2016) ^{225}Ac-PSMA-617 for PSMA-targeted α-radiation therapy of metastatic castration-resistant prostate cancer. J Nucl Med 57 (12):1941–1944
142. Kulkarni HR, Singh A et al (2018) Theranostics of prostate cancer: from molecular imaging to precision molecular radiotherapy targeting the prostate specific membrane antigen. Brit J Radiol 91:20180308
143. Kunikowska J1, Lewington V et al (2017) Optimizing somatostatin receptor imaging in patients with neuroendocrine tumors: the impact of ^{99m}Tc-HYNICTOC SPECT/SPECT/CT versus ^{68}Ga-DOTATATE PET/CT upon clinical management. Clin Nucl Med 42(12): 905–911
144. Kwekkeboom D, Krenning EP et al (2000) Peptide receptor imaging and therapy. J Nucl Med 41:1704–1713
145. La Bella R, Garcia-Garayoa E et al (2002) A ^{99m}Tc(I)-postlabeled high affinity bombesin analogue as a potential tumor imaging agent. Bioconjug Chem 13:599–604
146. Lantry LE, Cappelletti E et al (2006) ^{177}Lu-AMBA: synthesis and characterization of a selective ^{177}Lu-labeled GRP-R agonist for systemic radiotherapy of prostate cancer. J Nucl Med 47:1144–1152
147. Lawal IO, Ankrah AO et al (2017) Diagnostic sensitivity of Tc-99m HYNIC PSMA SPECT/CT in prostate carcinoma: a comparative analysis with Ga-68 PSMA PET/CT. Prostate 77:1205–1212

148. Lazarova L, Causey PW et al (2011) The synthesis, magnetic purification and evaluation of ^{99m}Tc-labeled microbubbles. Nucl Med Biol 38:1111–1118
149. Leamon CP, Parker MA et al (2002) Synthesis and biological evaluation of EC20: a new folate- derived, ^{99m}Tc-based radiopharmaceutical. Bioconjug Chem 13:1200–1210
150. Lei K, Rusckowski M et al (1996) Technetium-99m antibodies labeled with MAG_3 and SHNH: an in vitro and animal in vivo comparison. Nucl Med Biol 23:917–922
151. Leonidova A, Foerster C et al (2015) In vivo demonstration of an active tumor pretargeting approach with peptide nucleic acid bioconjugates as complementary system. Chem Sci 6:5601–5616
152. Leyton JV, Olafsen T et al (2008) Humanized radioiodinated minibody for imaging of prostate stem cell antigen-expressing tumors. Clin Cancer Res 14:7488–7496
153. Li M, Meares CF et al (1995) Prelabeling of chimeric monoclonal antibody L6 with 90yttrium- and 111indium-1,4,7,10-tetraazacyclododecane-N, N′, N″, N‴-tetraacetic acid (DOTA) chelates for radioimmunodiagnosis and therapy. Cancer Res 55:5726s–5728s
154. Lin X, Jin Z et al (2012) Synthesis and biodistribution of a New ^{99m}Tc-oxo complex with deoxyglucose dithiocarbamate for tumor imaging. Chem Biol Drug Des 79:239–245
155. Lindegren S, Frost SH (2011) Pretargeted radioimmunotherapy with α-particle emitting radionuclides. Curr Radiopharm 4:248–260
156. Liu G (2018) A revisit to the pretargeting concept–A target conversion. Front Pharmacol 9:1476
157. Liu S (2008) Bifunctional coupling agents for radiolabeling of biomolecules and target-specific delivery of metallic radionuclides. Adv Drug Deliv Rev 60:1347–1370
158. Liu S (2009) Radiolabeled cyclic RGD peptides as integrin alpha(v)beta(3)-targeted radiotracers: maximizing binding affinity via bivalency. Bioconjug Chem 20:2199–2213
159. Liu S, Edwards DS (1999) ^{99m}Tc-Labeled small peptides as diagnostic radiopharmaceuticals. Chem Rev 99:2235–2268
160. Liu S, Edwards DS et al (1998) A novel ternary ligand system for ^{99m}Tc-labeling of hydrazino nicotinamide-modified biologically active molecules using imine-N-containing heterocycles as coligands. Bioconjug Chem 9:583–595
161. Liu S, Kim YS et al (2008) Coligand effects on the solution stability, biodistribution and metabolism of the ^{99m}Tc-labeled cyclic RGDfK tetramer. Nucl Med Biol 35:111–121
162. Liu Z, Li ZB et al (2009) Small-animal PET of tumors with ^{64}Cu-labeled RGD-bombesin heterodimer. J Nucl Med 50:1168–1177
163. Liu Z, Niu G et al (2009) ^{68}Ga-labeled NOTA-RGD-BBN peptide for dual integrin and GRPR-targeted tumor imaging. Eur J Nucl Med Mol Imaging 36:1483–1494
164. Liu Z, Huang J et al (2012) ^{99m}Tc-labeled RGD-BBN peptide for small-animal SPECT/CT of lung carcinoma. Mol Pharm 9:1409–1417
165. Low PS, Henne WA et al (2008) Discovery and development of folic-acid-based receptor targeting for imaging and therapy of cancer and inflammatory diseases. Acc Chem Res 41:120–129
166. Lu G, Maresca KP et al (2013) Synthesis and SAR of ^{99m}Tc/Re-labeled small molecule prostate specific membrane antigen inhibitors with novel polar chelates. Bioorg Med Chem Lett 23:1557–1563
167. Lu J, Pang Y et al (2011) Synthesis and in vitro/in vivo evaluation of ^{99m}Tc-labeled folate conjugates for folate receptor imaging. Nucl Med Biol 38:557–565
168. Maddalena ME, Fox J et al (2009) ^{177}Lu-AMBA biodistribution, radiotherapeutic efficacy, imaging, and autoradiography in prostate cancer models with low GRP-R expression. J Nucl Med 50:2017–2024
169. Maes V, Garcia-Garayoa E et al (2006) Novel ^{99m}Tc-labeled neurotensin analogues with optimized biodistribution properties. J Med Chem 49:1833–1836
170. Maina T, Nikolopoulou A et al (2007) [^{99m}Tc]Demotensin 5 and 6 in the NTS1-R-targeted imaging of tumours: synthesis and preclinical results. Eur J Nucl Med Mol Imaging 34:1804–1814

171. Maina T, Nock B et al (2002) [^{99m}Tc]Demotate, a new ^{99m}Tc-based [Tyr^3]octreotate analogue for the detection of somatostatin receptor-positive tumours: synthesis and preclinical results. Eur J Nucl Med Mol Imaging 29:742–753
172. Mansi R, Wang X et al (2009) Evaluation of a 1,4,7,10-tetraazacyclododecane-1,4,7,10-tetraacetic acid-conjugated bombesin-based radioantagonist for the labeling with single-photon emission computed tomography, positron emission tomography, and therapeutic radionuclides. Clin Cancer Res 15:5240–5249
173. Mardirossian G, Wu C et al (1993) The stability in liver homogenates of indium-111 and yttrium-90 attached to antibody via two popular chelators. Nucl Med Biol 20:65–74
174. Maresca KP, Hillier SM et al (2009) Comprehensive radiolabeling, stability, and tissue distribution studies of technetium-99m single amino acid chelates (SAAC). Bioconjug Chem 20:1625–1633
175. Maresca KP, Hillier SM et al (2012) Small molecule inhibitors of PSMA incorporating technetium-99m for imaging prostate cancer: effects of chelate design on pharmacokinetics. Inorg Chim Acta 389:168–175
176. Maresca KP1, Hillier SM et al (2009) A series of halogenated heterodimeric inhibitors of prostate specific membrane antigen (PSMA) as radiolabeled probes for targeting prostate cancer. J Med Chem 52(2):347–357
177. Markwalder R, Reubi JC (1999) Gastrin-releasing peptide receptors in the human prostate: relation to neoplastic transformation. Cancer Res 59:1152–1159
178. Mather SJ, Nock BA et al (2014) GRP receptor imaging of prostate cancer using [$^{(99m)}$Tc]Demobesin 4: a first-in-man study. Mol Imaging Biol 16:888–895
179. Mathias CJ, Wang S et al (1998) Indium-111-DTPA-folate as a potential folate-receptor-targeted radiopharmaceutical. J Nucl Med 39:1579–1585
180. Matteson EL, Lowe VJ et al (2009) Assessment of disease activity in rheumatoid arthritis using a novel folate targeted radiopharmaceutical folatescan. Clin Exp Rheumatol 27:253–259
181. Maurer AH, Elsinga P et al (2014) Imaging the folate receptor on cancer cells with ^{99m}Tc-etarfolatide: properties, clinical use, and future potential of folate receptor imaging. J Nucl Med 55:701–704
182. Mercer JR, Xu LH et al (1989) Synthesis and tumor uptake of 5-^{82}Br- and 5-^{131}I-labeled 5-halo-1-(2-fluoro-2-deoxy-beta-D-ribofuranosyl)uracils. J Med Chem 32:1289–1294
183. Meredith RF, Buchsbaum DJ (2006) Pretargeted radioimmunotherapy. Int J Radiat Oncol Biol Phys 66:S57–S59
184. Mikołajczak R, Maecke HR (2016) Radiopharmaceuticals for somatostatin receptor imaging. Nucl Med Rev 19(2):126–132
185. Mindt TL, Jungi V et al (2008) Modification of different IgG1 antibodies via glutamine and lysine using bacterial and human tissue transglutaminase. Bioconjug Chem 19:271–278
186. Minko T, Paranjpe PV et al (2002) Enhancing the anticancer efficacy of camptothecin using biotinylated poly (ethylene glycol) conjugates in sensitive and multidrug-resistant human ovarian carcinoma cells. Cancer Chemother Pharmacol 50:143–150
187. Moody TW, Russell EK et al (1983) Bombesin-like peptides in small cell lung cancer: biochemical characterization and secretion from a cell line. Life Sci 32:487–493
188. Moreno P, Ramos-Álvarez I et al (2016) Bombesin related peptides/receptors and their promising therapeutic roles in cancer imaging, targeting and treatment. Expert Opin Ther Targets 20:1055–1073
189. Morris RT, Joyrich RN et al (2014) Phase II study of treatment of advanced ovarian cancer with folate-receptor-targeted therapeutic (vintafolide) and companion SPECT-based imaging agent (^{99m}Tc-etarfolatide). Ann Oncol 25:852–858
190. Müller C, Brühlmeier M et al (2006) Effects of antifolate drugs on the cellular uptake of radiofolates in vitro and in vivo. J Nucl Med 47:2057–2064

191. Müller C, Mindt TL et al (2009) Evaluation of a novel radiofolate in tumour-bearing mice: promising prospects for folate-based radionuclide therapy. Eur J Nucl Med Mol Imaging 36:938–946
192. Müller C, Reddy JA et al (2010) Effects of the antifolates pemetrexed and CB3717 on the tissue distribution of ^{99m}Tc-EC20 in xenografted and syngeneic tumor-bearing mice. Mol Pharm 7:597–604
193. Müller C, Schibli R et al (2008) Pemetrexed improves tumor selectivity of ^{111}In-DTPA-folate in mice with folate receptor-positive ovarian cancer. J Nucl Med 49:623–629
194. Müller C, Schubiger PA et al (2006) Synthesis and in vitro/in vivo evaluation of novel ^{99m}Tc $(CO)_3$-folates. Bioconjug Chem 17:797–806
195. Müller C, Schubiger PA et al (2007) Isostructural folate conjugates radiolabeled with the matched pair ^{99m}Tc/^{188}Re: a potential strategy for diagnosis and therapy of folate receptor-positive tumors. Nucl Med Biol 34:595–601
196. Müller C, Schibli R (2013) Prospects in folate receptor-targeted radionuclide therapy. Front Oncol 3:249
197. Müller C, Struthers H et al (2013) DOTA conjugate with an albumin-binding entity enables the first folic acid-targeted 177Lu-radionuclide tumor therapy in mice. J Nucl Med 54:124–131
198. Müller C (2013) Folate-based radiotracers for PET imaging-update and perspectives. Molecules 18:5005–5031
199. Müller C, Bunka M et al (2014) Promising prospects for ^{44}Sc-/^{47}Sc-based theragnostics: application of ^{47}Sc for radionuclide tumor therapy in mice. J Nucl Med 55:1658–1664
200. Müller C, Reber J et al (2014) Direct in vitro and in vivo comparison of ^{161}Tb and ^{177}Lu using a tumour-targeting folate conjugate. Eur J Nucl Med Mol Imaging 41:476–485
201. Müller C, Reber J et al (2014) Folate receptor targeted alpha-therapy using terbium-149. Pharmaceuticals 7:353–365
202. Munch-Petersen B, Cloos L et al (1995) Human thymidine kinase 1. regulation in normal and malignant cells. Adv Enzyme Regul 35:69–89
203. Narmani A, Yavari K et al (2017) Imaging, biodistribution and in vitro study of smart ^{99m}Tc-PAMAM G4 dendrimer as novel nano-complex. Coll Surf B 159:232–240
204. Neri D, Carnemolla B et al (1997) Targeting by affinity-matured recombinant antibody fragments of an angiogenesis associated fibronectin isoform. Nat Biotechnol 15:1271–1275
205. Nock B, Nikolopoulou A et al (2003) [^{99m}Tc]Demobesin 1, a novel potent bombesin analogue for GRP receptor-targeted tumour imaging. Eur J Nucl Med Mol Imaging 30:247–258
206. Nock BA, Nikolopoulou A et al (2005) Potent bombesin-like peptides for GRP-receptor targeting of tumors with ^{99m}Tc: a preclinical study. J Med Chem 48:100–110
207. Nock BA, Nikolopoulou A et al (2006) Toward stable N4-modified neurotensins for NTS1-receptor-targeted tumor imaging with ^{99m}Tc. J Med Chem 49:4767–4776
208. Núñez EG, Faintuch BL et al (2009) Influence of colloid particle profile on sentinel lymph node uptake. Nucl Med Biol 36:741–747
209. Oh P, Li Y et al (2004) Subtractive proteomic mapping of the endothelial surface in lung and solid tumours for tissue-specific therapy. Nature 429:629–635
210. Ozker K, Collier BD et al (1999) Biodistribution of ^{99m}Tc-labelled 5-thio-D-glucose. Nucl Med Commun 20:1055–1058
211. Papagiannopoulou D (2017) Technetium-99m radiochemistry for pharmaceutical applications. J Label Comp Radiopharm 60:502–520
212. Parker N, Turk MJ et al (2005) Folate receptor expression in carcinomas and normal tissues determined by a quantitative radioligand binding assay. Anal Biochem 338:284–293
213. Patra M, Zarschler K et al (2016) New insights into the pretargeting approach to image and treat tumours. Chem Soc Rev 45:6415–6431

214. Petrig J, Schibli R et al (2001) Derivatization of glucose and 2-deoxyglucose for transition metal complexation: substitution reactions with organometallic ^{99m}Tc and Re precursors and fundamental NMR investigations. Chemistry 7:1868–1873
215. Pini A, Viti F et al (1998) Design and use of a phage display library. human antibodies with subnanomolar affinity against a marker of angiogenesis eluted from a two-dimensional gel. J Biol Chem 273:21769–21776
216. Piramoon M, Hosseinimehr SJ (2016) The past, current studies and future of organometallic ^{99m}Tc(CO)$_3$ labeled peptides and proteines. Curr Pharm Des 22:4854–4867
217. Posey JA, Khazaeli MB et al (2001) A pilot trial of vitaxin, a humanized anti-vitronectin receptor (anti alpha v beta 3) antibody in patients with metastatic cancer. Cancer Biother Radiopharm 16:125–132
218. Pretze M, Wuest F et al (2010) The traceless Staudinger ligation with fluorine-18: a novel and versatile labeling technique for the synthesis of PET-radiotracers. Tetrahedron Lett 51:6410–6414
219. Purohit A, Liu S et al (2003) Phosphine-containing HYNIC derivatives as potential bifunctional chelators for ^{99m}Tc-labeling of small biomolecules. Bioconjug Chem 14:720–727
220. Rahbar K, Afshar-Oromieh A et al (2018) PSMA theranostics: current status and future directions. Mol Imaging 17:1536012118776068
221. Rahbar K, Ahmadzadehfar H et al (2017) German multicenter study investigating ^{177}Lu-PSMA-617 radioligand therapy in advanced prostate cancer patients. J Nucl Med 58:85–90
222. Reber J, Struthers H et al (2012) Radioiodinated folic acid conjugates: evaluation of a valuable concept to improve tumor-to-background contrast. Mol Pharm 9:1213–1221
223. Reddy JA, Xu LC et al (2004) Preclinical evaluation of ^{99m}Tc-EC20 for imaging folate receptor-positive tumors. J Nucl Med 45:857–866
224. Reubi JC, Waser B et al (1998) Neurotensin receptors: a new marker for human ductal pancreatic adenocarcinoma. Gut 42:546–550
225. Rezazadeh F, Sadeghzadeh N (2018) Tumor targeting with ^{99m}Tc radiolabeled peptides: clinical application and recent development. Chem Biol Drug Design. https://doi.org/10.1111/cbdd.13413
226. Retzloff L, Heinzke L et al (2010) Evaluation of [^{99m}Tc-(CO)$_3$-X-Y-Bombesin(7-14)NH$_2$] conjugates for targeting gastrin-releasing peptide receptors overexpressed on breast carcinoma. Anticancer Res 30:19–30
227. Risch VR, Honda T et al (1977) Distribution of ^{99m}Tc-1-thioglucose in rats: effect of administration route on pancreatic specificity. Radiology 124:837–838
228. Robu S, Schottelius M et al (2017) Preclinical evaluation and first patient application of ^{99m}Tc-PSMA-I&S for SPECT imaging and radioguided surgery in prostate cancer. J Nucl Med 58(2):235–242
229. Rolleman EJ, Valkema R et al (2003) Safe and effective inhibition of renal uptake of radiolabelled octreotide by a combination of lysine and arginine. Eur J Nucl Med Mol Imaging 30:9–15
230. Römhild K, Fischer CA, Mindt TL (2017) Glycated ^{99m}Tc-tricarbonyl-labeled peptide conjugates for tumor targeting by "Click-to-Chelate". ChemMedChem 12:66–74
231. Rosebrough SF (1993) Pharmacokinetics and biodistribution of radiolabeled avidin, streptavidin and biotin. Nucl Med Biol 20:663–668
232. Rowland DJ, Cherry SR (2008) Small-animal preclinical nuclear medicine instrumentation and methodology. Semin Nucl Med 38:209–222
233. Russell-Jones G, McTavish K et al (2004) Vitamin-mediated targeting as a potential mechanism to increase drug uptake by tumours. J Inorg Biochem 98:1625–1633
234. Salmaso S, Pappalardo JS et al (2009) Targeting glioma cells in vitro with ascorbate-conjugated pharmaceutical nanocarriers. Bioconjug Chem 20:2348–2355
235. Salouti M, Rajabi H et al (2008) Breast tumor targeting with ^{99m}Tc-HYNIC-PR81 complex as a new biologic radiopharmaceutical. Nucl Med Biol 35:763–768

236. Santimaria M, Moscatelli G et al (2003) Immunoscintigraphic detection of the ED-B domain of fibronectin, a marker of angiogenesis, in patients with cancer. Clin Cancer Res 9:571–579
237. Santos-Cuevas CL, Ferro-Flores G et al (2011) ^{99m}Tc-N_2S_2-Tat(49-57)-bombesin internalized in nuclei of prostate and breast cancer cells: kinetics, dosimetry and effect on cellular proliferation. Nucl Med Commun 32:303–313
238. Santos-Cuevas C, Davanzo J et al (2017) ^{99m}Tc-labeled PSMA inhibitor: biokinetics and radiation dosimetry in healthy subjects and imaging of prostate cancer tumors in patients. Nucl Med Biol 52:1–6
239. Schibli R, Dumas C et al (2005) Synthesis and in vitro characterization of organometallic rhenium and technetium glucose complexes against Glut 1 and hexokinase. Bioconjug Chem 16:105–112
240. Schibli R, La Bella R et al (2000) Influence of the denticity of ligand systems on the in vitro and in vivo behavior of ^{99m}Tc(I)-tricarbonyl complexes: a hint for the future functionalization of biomolecules. Bioconjug Chem 11:345–351
241. Schibli R, Schubiger PA (2002) Current use and future potential of organometallic radiopharmaceuticals. Eur J Nucl Med Mol Imaging 29:1529–1542
242. Schibli R, Schwarzbach R et al (2002) Steps toward high specific activity labeling of biomolecules for therapeutic application: preparation of precursor $[^{188}Re(H_2O)_3(CO)_3]^+$ and synthesis of tailor-made bifunctional ligand systems. Bioconjug Chem 13:750–756
243. Schmid M, Neumaier B et al (2006) Synthesis and evaluation of a radiometal-labeled macrocyclic chelator-derivatised thymidine analog. Nucl Med Biol 33:359–366
244. Schmidkonz C, Cordes M et al (2018) SPECT/CT with the PSMA ligand ^{99m}Tc-MIP-1404 for whole-body primary staging of patients with prostate cancer. Clin Nucl Med 43:225–231
245. Schmidkonz C, Hollweg C et al (2018) ^{99m}Tc-MIP-1404-SPECT/CT for the detection of PSMA-positive lesions in 225 patients with biochemical recurrence of prostate cancer. Prostate 78:54–63
246. Schottelius M, Laufer B et al (2009) Ligands for mapping alphavbeta3-integrin expression in vivo. Acc Chem Res 42:969–980
247. Schottelius M, Wester HJ (2009) Molecular imaging targeting peptide receptors. Methods 48:161–177
248. Schottelius M, Wester HJ et al (2002) Improvement of pharmacokinetics of radioiodinated Tyr^3-octreotide by conjugation with carbohydrates. Bioconjug Chem 13:1021–1030
249. Schubert M, Foerster C et al (2017) A novel tumor pretargeting system based on complementary L-configured oligonucleotides. Biocon Chem 28:1176–1188
250. Schwartz DA, Abrams MJ et al (1991) Preparation of hydrazino-modified proteins and their use for the synthesis of ^{99m}Tc-protein conjugates. Bioconjug Chem 2:333–336
251. Schweinsberg C, Maes V et al (2008) Novel glycated $[^{99m}Tc(CO)_3]$-labeled bombesin analogues for improved targeting of gastrin-releasing peptide receptor-positive tumors. Bioconjug Chem 19:2432–2439
252. Seetharam B (1999) Receptor-mediated endocytosis of cobalamin (vitamin B_{12}). Annu Rev Nutr 19:173–195
253. Seetharam B, Li N (2000) Transcobalamin II and its cell surface receptor. Vitam Horm 59:337–366
254. Seetharam B, Yammani RR (2003) Cobalamin transport proteins and their cell-surface receptors. Expert Rev Mol Med 5:1–18
255. Semnani ES, Wang K et al (2005) 5-[^{123}I/^{125}I]iodo-2′-deoxyuridine in metastatic lung cancer: radiopharmaceutical formulation affects targeting. J Nucl Med 46:800–806
256. Shariati F, Aryana K et al (2014) Diagnostic value of ^{99m}Tc-bombesin scintigraphy for differentiation of malignant from benign breast lesions. Nucl Med Commun 35:620–625
257. Sharkey RM, Karacay H et al (2005) Improving the delivery of radionuclides for imaging and therapy of cancer using pretargeting methods. Clin Cancer Res 11:7109s
258. Sharp SE, Trout AT et al (2016) MIBG in neuroblastoma diagnostic imaging and therapy. RadioGraphics 36:258–278

259. Shi J, Kim YS et al (2009) Improving tumor uptake and pharmacokinetics of ^{64}Cu-labeled cyclic RGD peptide dimers with Gly(3) and PEG(4) linkers. Bioconjug Chem 20:750–759
260. Shi J, Wang L et al (2008) Improving tumor uptake and excretion kinetics of ^{99m}Tc-labeled cyclic arginine-glycine-aspartic (RGD) dimers with triglycine linkers. J Med Chem 51:7980–7990
261. Siegel BA, Dehdashti F et al (2003) Evaluation of ^{111}In-DTPA-folate as a receptor-targeted diagnostic agent for ovarian cancer: initial clinical results. J Nucl Med 44:700–707
262. Silver DA, Pellicer I et al (1997) Prostatespecific membrane antigen expression in normal and malignant human tissues. Clin Cancer Res 3:81–85
263. Silvestri C, Christopher A et al (2019) Consecutive case series of melanoma sentinel node biopsy for lymphoseek compared to sulfur colloids. J Surg Res 233:149–153
264. Siwowska K, Müller C (2015) Preclinical development of small-molecular-weight folate-based radioconjugates: a pharmacological perspective. Quart J Nucl Med Mol Imaging 59:269–286
265. Smith CJ, Gali H et al (2003) Radiochemical investigations of ^{177}Lu-DOTA-8-Aoc-BBN [7-14]NH_2: an in vitro/in vivo assessment of the targeting ability of this new radiopharmaceutical for PC-3 human prostate cancer cells. Nucl Med Biol 30:101–109
266. Smith CJ, Sieckman GL et al (2003) Radiochemical investigations of gastrin-releasing peptide receptor-specific [^{99m}Tc(X)$(CO)_3$-Dpr-Ser-Ser–Ser-Gln-Trp-Ala-Val-Gly-His-Leu-Met-(NH_2)] in PC-3, tumor-bearing, rodent models: syntheses, radiolabeling, and in vitro/in vivo studies where Dpr = 2,3-diaminopropionic acid and X = H_2O or $P(CH_2OH)_3$. Ca Cancer Res 63:4082–4088
267. Smith CJ, Sieckman GL et al (2003) Radiochemical investigations of [^{188}Re(H_2O)$(CO)_3$-diaminopropionic acid-SSS-bombesin(7-14)NH2]: syntheses, radiolabeling and in vitro/in vivo GRP receptor targeting studies. Anticancer Res 23:63–70
268. Smith CJ, Volkert WA et al (2003) Gastrin releasing peptide (GRP) receptor targeted radiopharmaceuticals: a concise update. Nucl Med Biol 30:861–868
269. Smith CJ, Volkert WA et al (2005) Radiolabeled peptide conjugates for targeting of the bombesin receptor superfamily subtypes. Nucl Med Biol 32:733–740
270. Smith TAD (2001) The rate-limiting step for tumor [^{18}F]fluoro-2-deoxy-D-glucose (FDG) incorporation. Nucl Med Biol 28:1–4
271. Sosabowski JK, Matzow T et al (2009) Targeting of CCK-2 receptor-expressing tumors using a radiolabeled divalent gastrin peptide. J Nucl Med 50:2082–2089
272. Spanoudaki VC, Ziegler SI (2008) PET and SPECT instrumentation. Handb Exp Pharmacol 185:53–74
273. Steen EJL, Edem PE et al (2018) Pretargeting in nuclear imaging and radionuclide therapy: improvingefficacy of theranostics and nanomedicines. Biomaterials 179:209–245
274. Steffens MG, Oosterwijk E et al (1999) In vivo and in vitro characterizations of three ^{99m}Tc-labeled monoclonal antibody G250 preparations. J Nucl Med 40:829–836
275. Storr T, Fisher CL et al (2005) A glucosamine-dipicolylamine conjugate of ^{99m}Tc(I) and ^{186}Re(I) for use in imaging and therapy. Dalton Trans 21(4):654–655
276. Struthers H, Hagenbach A et al (2009) Organometallic $[Re(CO)_3]^+$ and $[Re(CO)_2(NO)]^{2+}$ labeled substrates for human thymidine kinase 1. I. Inorg Chem 48:5154–5163
277. Struthers H, Spingler B et al (2008) "Click-to-chelate": design and incorporation of triazole-containing metal-chelating systems into biomolecules of diagnostic and therapeutic interest. Chemistry 14:6173–6183
278. Surasi DS, O'Malley J et al (2015) ^{99m}Tc-Tilmanocept: a novel molecular agent for lymphatic mapping and sentinel lymph node localization. J Nucl Med Technol 43:87–91
279. Tang Y, Scollard D et al (2005) Imaging of HER2/neu expression in BT-474 human breast cancer xenografts in athymic mice using [^{99m}Tc]-HYNIC-trastuzumab (Herceptin) Fab fragments. Nucl Med Commun 26:427–432
280. Tienken L, Drude N et al (2018) Evaluation of a pretargeting strategy for molecular imaging of the prostate stem cell antigen with a single chain antibody. Sci Rep 8:3755

281. Tolmachev V, Friedman M et al (2009) Affibody molecules for epidermal growth factor receptor targeting in vivo: aspects of dimerization and labeling chemistry. J Nucl Med 50:274–283
282. Torizuka T, Tamaki N et al (1995) In vivo assessment of glucose metabolism in hepatocellular carcinoma with FDG-PET. J Nucl Med 36:1811–1817
283. Toyohara J, Hayashi A et al (2002) Rationale of 5-^{125}I-iodo-4′-thio-2′-deoxyuridine as a potential iodinated proliferation marker. J Nucl Med 43:1218–1226
284. Toyohara J, Hayashi A et al (2003) Development of radioiodinated nucleoside analogs for imaging tissue proliferation: comparisons of six 5-iodonucleosides. Nucl Med Biol 30:687–696
285. Trogrlic M, Tezak S (2016) ^{99m}Tc-EDDA/HYNIC-TOC in management of patients with head and neck somatostatin receptor positive tumors. Nucl Med Rev 19:74–80
286. Unkart JT, Wallace AM (2017) Use of ^{99m}Tc-tilmanocept as a single agent for sentinel lymph node identification in breast cancer: a retrospective pilot study. J Nucl Med Technol 45:181–184
287. Vallabhajosula S, Nikolopoulou A et al (2014) ^{99m}Tc-labeled small-molecule inhibitors of prostate-specific membrane antigen: pharmacokinetics and biodistribution studies in healthy subjects and patients with metastatic prostate cancer. J Nucl Med 55:1791–1798
288. Van de Wiele C, Dumont F et al (2000) Technetium-99m RP527, a GRP analogue for visualisation of GRP receptor-expressing malignancies: a feasibility study. Eur J Nucl Med 27:1694–1699
289. van der Kroon I, Joosten L et al (2016) Improved quantification of the beta cell mass after pancreas visualization with ^{99m}Tc-demobesin-4 and beta cell imaging with ^{111}In-exendin-3 in rodents. Mol Pharm 13:3478–3483
290. van der Poel HG, Buckle T et al (2011) Intraoperative laparoscopic fluorescence guidance to the sentinel lymph node in prostate cancer patients: clinical proof of concept of an integrated functional imaging approach using a multimodal tracer. Eur Urol 60:826–833
291. Varasteh Z, Hyafil F et al (2017) Targeting mannose receptor expression on macrophages in atherosclerotic plaques of apolipoprotein E-knockout mice using ^{111}In-tilmanocept. EJNMMI Res 7:40
292. Vera DR, Wallace AM et al (2001) A synthetic macromolecule for sentinel node detection: ^{99m}Tc-DTPA-Mannosyl-dextran. J Nucl Med 42:951–959
293. Verhaar-Langereis MJ, Zonnenberg BA et al (2000) Radioimmunodiagnosis and therapy. Cancer Treat Rev 26:3–10
294. Verwijnen SM, Krenning EP et al (2005) Oral versus intravenous administration of lysine: equal effectiveness in reduction of renal uptake of [^{111}In-DTPA]octreotide. J Nucl Med 46:2057–2060
295. Vidal-Sicart S, Vera DR et al (2018) Next generation of radiotracers for sentinel lymph node biopsy: What is still necessary to establish new imaging paradigms? Rev Esp Med Nucl Imagen Mol 37:373–379
296. von Guggenberg E, Dietrich H et al (2007) ^{99m}Tc-labelled HYNIC-minigastrin with reduced kidney uptake for targeting of CCK-2 receptor-positive tumours. Eur J Nucl Med Mol Imaging 34:1209–1218
297. Vöö S, Bucerius J et al (2011) I-131-MIBG therapies. Methods 55(3):238–245
298. Waibel R, Treichler H et al (2008) New derivatives of vitamin B_{12} show preferential targeting of tumors. Cancer Res 68:2904–2911
299. Wang L, Shi J et al (2009) Improving tumor-targeting capability and pharmacokinetics of ^{99m}Tc-labeled cyclic RGD dimers with PEG(4) linkers. Mol Pharm 6:231–245
300. Wang S, Luo J et al (1997) Design and synthesis of [^{111}In]DTPA-folate for use as a tumor-targeted radiopharmaceutical. Bioconjug Chem 8:673–679
301. Wang Y, Zhu J et al (2014) Synthesis and evaluation of ^{99m}Tc–2-[(3-carboxy-1-oxopropyl) amino]-2-deoxy-D-glucose as a potential tumor imaging agent. Bioorg Med Chem Lett 24:3882–3885

302. Wängler C, Schirrmacher R et al (2009) Simple and convenient radiolabeling of proteins using a prelabeling-approach with thiol-DOTA. Bioorg Med Chem Lett 19:1926–1929
303. Weineisen M, Šimeček J et al (2014) Synthesis and preclinical evaluation of DOTAGA-conjugated PSMA ligands for functional imaging and endoradiotherapy of prostate cancer. EJNMMI Res 4:63
304. Weitman SD, Lark RH et al (1992) Distribution of the folate receptor GP38 in normal and malignant cell lines and tissues. Cancer Res 52:3396–3401
305. Wester HJ, Schottelius M et al (2002) Comparison of radioiodinated TOC, TOCA and Mtr-TOCA: the effect of carbohydration on the pharmacokinetics. Eur J Nucl Med Mol Imaging 29:28–38
306. Wieland DM, Wu J et al (1980) Radiolabeled adrenergi neuron-blocking agents: adrenomedullary imaging with [^{131}I]iodobenzylguanidine. J Nucl Med 21:349–353
307. Wilbur DS, Hamlin DK et al (1996) Synthesis and nca-radioiodination of arylstannyl-cobalamin conjugates. evaluation of aryliodo-cobalamin conjugate binding to transcobalamin II and biodistribution in mice. Bioconjug Chem 7:461–474
308. Wilbur DS, Hamlin DK et al (1998) Synthesis and evaluation of ^{99m}Tc/^{99}Tc-MAG$_3$-biotin conjugates for antibody pretargeting strategies. Nucl Med Biol 25:611–619
309. Xu N, Cai G et al (2009) Molecular imaging application of radioiodinated anti-EGFR human Fab to EGFR-overexpressing tumor xenografts. Anticancer Res 29:4005–4011
310. Yamada Y, Nakatani H et al (2015) Phase I clinical trial of ^{99m}Tc-etarfolatide, an imaging agent for folate receptor in healthy Japanese adults. Ann Nucl Med 29:792–798
311. Yang W, Cheng Y et al (2009) Targeting cancer cells with biotin-dendrimer conjugates. Eur J Med Chem 44:862–868
312. Yim CB, Boerman OC et al (2009) Versatile conjugation of octreotide to dendrimers by cycloaddition ("click") chemistry to yield high-affinity multivalent cyclic peptide dendrimers. Bioconjug Chem 20:1323–1331
313. Yokota T, Milenic DE et al (1992) Rapid tumor penetration of a single-chain Fv and comparison with other immunoglobulin forms. Cancer Res 52:3402–3408
314. Yokota T, Milenic DE et al (1993) Microautoradiographic analysis of the normal organ distribution of radioiodinated single-chain Fv and other immunoglobulin forms. Cancer Res 53:3776–3783
315. Zardi L, Carnemolla B et al (1987) Transformed human cells produce a new fibronectin isoform by preferential alternative splicing of a previously unobserved exon. EMBO J 6:2337–2342
316. Zechmann CM, Afshar-Oromieh A et al (2014) Radiation dosimetry and first therapy results with a ^{124}I/^{131}I-labeled small molecule (MIP-1095) targeting PSMA for prostate cancer therapy. Eur J Nucl Med Mol Imaging 41:1280–1292
317. Zelenka K, Lubor Borsig L, Alberto R (2011) Trifunctional ^{99m}Tc based radiopharmaceuticals: metal-mediated conjugation of a peptide with a nucleus targeting intercalator. Org Biomol Chem 9:1071–1078
318. Zeltchan R, Medvedeva A et al (2016) Experimental study of radiopharmaceuticals based on technetium-99m labeled derivative of glucose for tumor diagnosis. IOP Conf Ser: Mater Sci Eng 135:012054
319. Zhang J, Ren J (2009) Synthesis and biological evaluation of a novel ^{99m}Tc nitrido radiopharmaceutical with deoxyglucose dithiocarbamate, showing tumor uptake. Bioorg Med Chem Lett 19:2752–2754
320. Zhang H, Chen J et al (2004) Synthesis and evaluation of bombesin derivatives on the basis of pan-bombesin peptides labeled with indium-111, lutetium-177, and yttrium-90 for targeting bombesin receptor-expressing tumors. Cancer Res 64:6707–6715
321. Zhang Y, Sun Y et al (2010) Radiosynthesis and micro-SPECT imaging of ^{99m}Tc-dendrimer poly(amido)-amine folic acid conjugate. Bioorg Med Chem Lett 20:927–931
322. Zwanziger D, Khan IU et al (2008) Novel chemically modified analogues of neuropeptide Y for tumor targeting. Bioconjug Chem 19:1430–1438